EVALUATION OF THE EFFECTS OF RESIDUAL SURFACE COMPRESSION ON THE STRENGTH OF STRUCTURAL GLASS BOLTED CONNECTIONS

A Thesis

by

RIGERS BEJKOLLARI

Submitted to the Office of Graduate and Professional Studies of
Texas A&M University
in partial fulfillment of the requirements for the degree of

MASTER OF SCIENCE

Chair of Committee,	W. Lynn Beason
Committee Members,	Zenon Medina-Cetina
	Robert Warden
Head of Department,	Robin Autenrieth

May 2018

Major Subject: Civil Engineering

ABSTRACT

In the recent years, glass has become the material of choice for glazing of building facades. Spider fittings are a popular method for the connection and support of glass plates that are part of the building façade. This application requires the design of glass plates with mounting holes. To increase the strength of glass plates used in glazing applications, residual surface compressive stresses are often induced into the plates through heat-treatment. In designing these connections, engineers have often assumed that the ultimate strength of a glass plate equals the strength of the pre-heat-treated plate combined with the amount of residual surface compression induced during heat-treatment. The focus of this thesis is to understand if this concept is conservative for the design of structural glass bolted connections.

This thesis studied the combined effects of the residual surface compression, localized stress concentration, and mounting hole-edge surface flaw condition on the strength of structural glass bolted connections. The focus was to develop an understanding of how the residual surface compression affects the strength of glass around a mounting hole, for a given geometry and edge condition. This was done by experimentally evaluating the strength of glass plate specimens with varying levels of residual surface compression. All specimens had identical geometry and a centered mounting hole with a constant diameter. Experimentally recorded ultimate loads were

converted to ultimate stresses using finite element analysis (FEA). Values of ultimate stress were then adjusted to generate equivalent 3-second load duration failure stresses.

It is concluded that for the glass specimens tested herein, estimating the ultimate strength of heat-treated glass as the strength of pre-heat-treated glass combined with the amount of residual surface compression induced during heat-treatment yields to a conservative design. The possible effects of residual surface compression, combined with stress concentrations around the mounting hole, and the hole-edge surface conditions are also shown. Lastly, this thesis gives recommendations for further research on this topic.

DEDICATION

To my grandparents, Xhevair and Shqiponja Mersinaj, for wanting to make them proud inspires me every day.

To my family, Perparim, Klarida, and Andi Bejkollari, for their unconditional love and encouragement.

To my wife Adelina Kaza and her family, because her ever-lasting love and support made the writing of this thesis possible.

ACKNOWLEDGEMENTS

First and foremost, I would like to thank my committee chair, Dr. W. Lynn Beason, and my committee members, Dr. Zenon Medina-Cetina, and Dr. Robert Warden for their guidance and support in the preparation of this thesis.

A special thanks goes towards Dr. Michael S. Brackin and Mr. A. William Lingnell for their contributions and technical advice given during the development of this research. In addition, thanks go to Mr. James C. Kovar, Mr. Sofokli Cakalli, and Mr. Sana Moran for their assistance in preparing for the physical testing that was performed as part of this research.

Finally, thanks to my wife, Adelina, for her patience and love while performing this research and writing this thesis.

CONTRIBUTORS AND FUNDING SOURCES

Contributors

This work was supervised by a committee consisting of Professors W. Lynn Beason and Zenon Medina-Cetina of the Zachry Department of Civil Engineering and Professor Robert Warden of the Department of Architecture.

All of the work performed as part of the thesis was completed independently by the student.

Funding Sources

This work was made possible, in part, by Beason Brackin & Associates, LLC and TriStar Glass, Inc.

The contents of this thesis are solely the responsibility of the author and do not necessarily represent the official views of Beason Brackin & Associates, LLC or TriStar Glass, Inc.

NOMENCLATURE

E	Young's Modulus
FEA	Finite Element Analysis
f_{AG}	Strength of Annealed Glass
f_{TG}	Strength of Fully Tempered Glass
G	Shear Modulus
I	Cross-sectional Moment of Inertia
K	Bulk Modulus
Kf	Glass Resistance to Failure
K_t	Stress Concentration Factor
P	Applied Point Load
R	Deflection Factor
t_d	Load Duration Time
t_f	Failure Load Duration Time
$w(z)$	Uniform Area Pressure
σ_{ANN-H}	Ultimate Stress of Annealed Glass w/ Mounting Hole
σ_{FT-H}	Ultimate Stress of Fully Tempered Glass w/ Mounting Hole
σ_{HS-H}	Ultimate Stress of Heat-strengthened Glass w/ Mounting Hole
σ_{max}	Maximum Bending Stress
σ_{rc}^{min}	Minimum Mounting Hole Residual Surface Compression

$\lvert\sigma_{surf}\rvert$	Residual Surface Compression
$\sigma(t)$	Nominal Tensile Stress
$\tilde{\sigma}_{td}$	Mean Failure Stress of a Given Loading Duration Time
σ_{∞}	Nominal Residual Surface Compression
δ_{max}	Maximum Deflection
υ	Poisson's Ratio
μ	Friction Coefficient

TABLE OF CONTENTS

Page

LIST OF FIGURES

Page

LIST OF TABLES

Page

1. INTRODUCTION

In the recent years, glass has become the material of choice for several building applications. One of the most common applications of structural glass is the glazing of building facades. There are many methods of supporting glass plates that are part of a curtain wall system; however, one method in particular, which involves glass plates being attached to supporting frames with spider fittings that go through circular mounting holes, has become increasingly popular among architects (Khoraskani, 2015). An obvious reason for this is the impression of an unobstructed glass façade that is created when connecting glass plates with spider fittings. While this method of glass support has become more popular, there is a large amount of uncertainty associated with the structural design of glass bolted connections. This uncertainty is mainly associated with three factors that tend to drive the design of structural glass bolted connections: the residual surface compression that originates from the heat-treatment of glass plates, the localized stress concentration caused by drilling the mounting hole, and the hole-edge surface condition. Traditionally, engineers have assumed that the ultimate strength of a heat-treated glass plate is equal to the strength of the pre-heat treated plate combined with the amount of residual surface compression induced during heat-treatment. The focus of this thesis is to understand if this concept is conservative for the design of glass plates with mounting holes.

The following paragraphs show a detailed description of the three factors that affect the strength of structural glass bolted connections. The next paragraphs present the problem discussed herein, and the experimental methods used to solve it. Following that, the importance of obtaining an adequate design of structural glass bolted connections is

emphasized. At the end of this introduction, a general overview of the sections that comprise this thesis is given.

One of the factors that affects the strength of glass plates with mounting holes is the residual surface compression. With the increase in the scope of structural glass applications throughout the years, glass manufactures have been striving to enhance the strength of glass plates. An effective method of increasing the strength of glass plates is to subject them to a heat-treatment process that induces residual surface and edge compressions. Most glass plates with mounting holes that are part of building facades are subjected to this heat-treatment. The presence of mounting holes in glass plates subjected to heat-treatment may alter the amount of heat-treatment, and thus, the levels of surface compression that the hole-edge surface receives (Nielsen, et al., 2009).

Another factor that affects the strength of a glass plate with a mounting hole is the localized stress concentration caused by drilling the hole. A mounting hole introduces a discontinuity in the surface of the glass plate. Stresses originating from external loads tend to concentrate around these discontinuities. Thus, for a given loading and support condition, a glass plate with a mounting hole experiences stresses that are several times higher than the stresses on the same plate without a hole. Engineers and glass designers have historically relied on tabulated values of stress concentrations for a variety of plate geometries with circular holes, subjected to typical loading and support conditions (Peterson, 1974). However, with the increased spectrum of the application of structural glass, engineers often encounter design problems with geometries and loading conditions that may not be accounted for in the traditional studies of stress concentration factors. In such cases, engineers either attempt to extrapolate stress concentration factors from

existing charts to the situation at hand, or use finite element analysis (FEA) to perform stress concentration studies that are tailored to the specific plate geometry, and loading and support conditions.

The third factor that affects the strength of glass plates with mounting holes is the distribution of surface flaws in the immediate vicinity of the mounting hole, which in this thesis is also referred to as the hole-edge surface condition. The act of drilling a mounting hole in a glass plate introduces flaws around the perimeter and the surface of the mounting hole. These flaws are often visible, extremely difficult to quantify, and introduce a large amount of uncertainty in the design of structural glass bolted connections (Lindqvist, 2013).

While these factors have already been studied individually, and design recommendations that account for their effects on the strength of glass can be found in the literature (Peterson, 1974; Beason, 1980; Beason and Morgan, 1984; Beason, et al, 1998; Nielsen, et al, 2009; Lindqvist, 2013), there is no study that accounts for the combined effects of the residual surface compression, the localized stress concentration, and the hole-edge surface condition to the strength of structural glass bolted connections.

This research studied the effects of residual surface compression on the strength of glass plates with mounting holes, for a given hole geometry and edge condition. Structural glass plates with varying levels of residual surface compression were subjected to destructive testing and their experimental ultimate loads were recorded. The varying levels of residual surface compression were estimated using a Grazing Angle Surface Polarimeter (GASP). The GASP is a well-recognized instrument for measuring the residual surface compressions. All specimens tested had identical geometry and centered

mounting holes with constant diameter, which assured a constant stress concentration factor and hole-edge condition throughout the experiment. FEA was utilized to estimate stress concentration factors that were applicable to the glass plates being tested. The geometric nonlinear FEA models of glass plates with mounting holes were used to determine the behavior of glass plates. FEA was used to calculate ultimate stress values based on the experimentally recorded ultimate loads for the glass specimens tested. The calculated ultimate stresses were adjusted to produce equivalent 3-second load duration failure stresses. Through this procedure, a relationship between the residual surface compression and the strength of the tested specimens was examined.

The proper design of structural glass bolted connections is extremely important to the overall performance of a building. Glass facades are often the first-and-only barrier of protection to the interior parts of a structure. In case of failure, extreme wind loads can not only directly risk the life of people, but also introduce undesirable dynamic effects to a structure. In addition to presenting safety and structural problems, poor design of structural glass can result in large economical costs to a project. It is also speculated that several glass manufacturers avoid the promotion of structural glass due to fear of liability (Davidson, 2000). This research contributes to the existing knowledge in the field of structural glass by investigating the adequacy of glass design concepts for the design of structural glass bolted connections.

The following section introduces in detail the problem considered herein, and the research procedure used to solve it. Section 3 presents a review of pertinent literature related to the factors that affect the design of structural glass bolted connections. Section 4 describes the experimental effort, and section 5 provides the evaluation of the

experimental results. Conclusions of this thesis, along with recommendations for future research related to the design of structural glass bolted connections are presented in section 6.

2. PROBLEM STATEMENT

2.1. Problem Background & Significance

Structural glass bolted connections are extensively utilized in structural glazing curtain wall systems. A typical structural glass bolted connection consists of a stainless-steel spider fitting that attaches glass plates to a supporting system. The stainless-steel spider fitting connects to the glass using a bolt that passes through the padded glass mounting hole. The bolt is fastened in place by a nut on the opposite side of the glass. The supporting system, which can be designed of glass, steel, or other materials, transfers the external loads from the façade to the frame of the building. Figure 1 presents a typical structural glass bolted connection.

Figure 1. Bolted Structural Glazing (reprinted from Khoraskani, 2015)

Based on existing knowledge related to the topic of structural glass, it is believed that there are three primary glass-related factors that control the strength of a glass bolted connection: the residual surface compression in the vicinity of the mounting hole, the localized stress concentration caused by drilling the mounting hole, and the hole-edge condition. The following paragraphs provide a brief explanation of each of these three factors.

The residual surface compression originates from the heat treatment of annealed float glass. Almost every type of flat glass in use today originates as annealed float glass, which is often referred to as simply annealed glass. During the heat treatment process, annealed glass is heated near its softening point, and then quickly quenched. In the quenching process, the outer surfaces of the glass are air blasted and cooled at a faster rate than its interior. This causes the surface of the glass to become rigid, while the interior remains soft. When the interior of glass eventually cools, a residual surface compression and an interior tensile stress distribution are locked into the glass. The presence of residual surface compression effectively increases the strength of annealed glass because mechanical tensile stresses induced in the glass surface have to overcome the residual surface compression, before the surface of glass experiences a net tensile stress. The heat-treatment process is often controlled to develop two different types of heat-treated glass: heat-strengthened and fully tempered glass (Beason and Lingnell, 2000). By definition, fully tempered glass has a higher residual surface compression, and hence, higher ultimate strength, than heat-strengthened glass. Heat-strengthened and fully tempered glass both have higher strength than annealed glass (ASTM, 1997a).

The localized stress concentration in a structural glass bolted connection is attributed to the mere presence of the mounting hole in the glass plate. The hole introduces a discontinuity to the stress flow in the plate, causing stresses to concentrate around the edge of the hole. Previous studies of stress concentration factors have indicated that for a given loading and support condition, the stress on a rectangular plate with a hole is generally 2-3 times higher than the stress on the same plate without a hole. Stress concentration factors around a mounting hole vary based on the plate's geometry, the hole diameter, and the loading conditions (Peterson, 1974).

Drilling of mounting holes in annealed glass plates introduces a population of flaws around the edge of the hole. The production of heat-strengthened and fully tempered glass starts with the uniform heating of annealed glass plates with pre-drilled mounting holes, and ends with the sudden quenching of glass. Mounting holes are drilled when glass is in the annealed float stage because of the low residual surface compressive stresses present in annealed glass, and any attempt to drill a mounting hole in heat-treated glass will likely result in the complete shattering of the glass specimen. The dimensions of flaws along the edge of mounting holes range from microscopic to visible. These flaws significantly affect the strength of glass (Beason, 1980; Beason and Morgan, 1984; Beason, et al, 1998).

When designing heat-treated window glass, engineers have traditionally assumed that the ultimate strength of a particular glass plate is equal to the strength of the annealed plate of the same geometry combined with the amount of residual surface compression induced in the annealed plate during heat-treatment. In the case of structural glass bolted connections, it is reasonable to believe that the presence of a mounting hole in an

annealed glass plate entering the heat-treatment process, causes the surface of glass around the hole to cool at a different rate, and thus, have different levels of residual surface compression than the surface of glass away from the hole.

In this study, glass test specimens were selected so that the localized stress concentration and hole-edge flaw condition were held constant. Therefore, the focus of this research was to develop an understanding of how the residual surface compression affects the strength of glass around a mounting hole, for the given hole geometry and edge condition. The primary focus of this thesis is to determine if the traditional concept used in the design of heat treated window glass is conservative for the design of structural glass bolted connections.

2.2. Research Aim & Procedure

This study is focused on developing an understanding of how the residual surface compression affects the strength of glass around a mounting hole, for a given hole geometry and edge condition. For this reason, annealed, heat strengthened, and fully tempered glass plates were tested. The glass plates were fabricated with ¼ inch glass that had planar dimensions of 16 x 16 inch. Each specimen had a drilled 1-7/16 inch diameter centered hole. The selection of this plate geometry and hole diameter was done to keep the stress concentration and surface edge-condition around the hole constant throughout this study. Specimens were subjected to a unique loading condition that induced a uniform biaxial stress in the immediate vicinity of the mounting hole.

All glass specimens tested were subject to the same initial fabrication procedure. Photographs of the hole-edge surface condition were taken for each specimen tested. Based on an unmagnified visual inspection, the hole-edge surface condition was

determined to be essentially the same for all heat-strengthened and fully tempered specimens. It is known that any randomly occurring severe flaws induced around the surface of a mounting hole during the drilling process in annealed glass might cause spontaneous breakage of the glass when it is subjected to the heating and quenching associated with the heat-treatment process. This phenomenon could cause an apparent increase in strength of heat-strengthened glass specimens due to the failure of the "weaker siblings" during the heat-treatment process. Records of spontaneous breakage of the glass during the treatment process were not maintained by the glass fabricator. However, it seems likely that the hole-edge flaws that survived the heat treatment process would be less severe than the flaws associated with the annealed specimens. While this effect cannot be easily quantified, it needs to be considered in the data interpretation discussed later in this thesis.

To evaluate the stress concentration factors applicable to this study, results from previous studies of stress concentrations were considered, and are summarized in the literature review. While these studies present comprehensive lists of stress concentration factors for plates with circular holes, the conditions presented in the literature do not match the exact geometry, loading, and support conditions considered herein (Figure 2). Therefore, ANSYS, a commercial FEA software, was utilized to evaluate the magnitude of stresses around the mounting hole, for the given geometry and loading condition. ANSYS was used to develop charts that relate the applied loads and the maximum tensile stress around the inner edge of the hole. Ultimate load data for each heat-treated specimen were converted to ultimate stress data using FEA generated load vs stress

charts. In this way the magnitudes of the localized stress concentration factors were accounted for, without being directly measured.

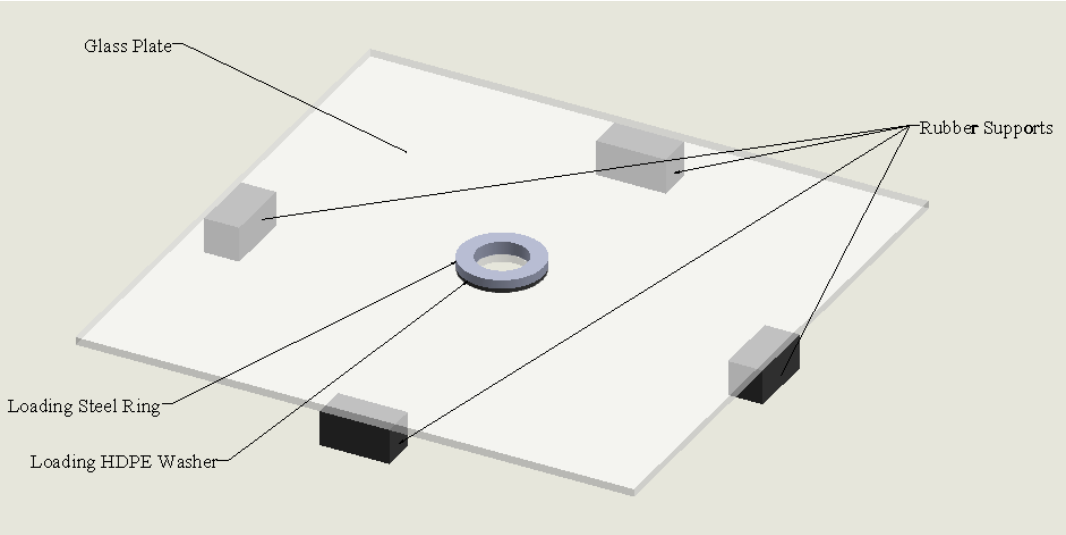

Figure 2. Sketch of Specimen Support and Loading Condition

For practical reasons, commonly available instruments do not allow for the measurement of the magnitude of the residual surface compression in the immediate vicinity of a mounting hole. Based on the uneven cooling rates that must occur in the vicinity of the hole, it seems reasonable to believe that the residual surface compression measured away from a mounting hole differs from the residual surface compression near the mounting hole. Residual surface compression measurements presented in this thesis refer to the residual surface compression measured at a location away from the mounting hole, and is referred to as the nominal residual surface compression. The nominal residual surface compression in the heat-strengthened and fully tempered glass specimens was

measured used a Grazing Angle Surface Polarimeter (GASP). More information about the GASP is provided in the later sections of this thesis.

To summarize, there are three factors that determine the strength of a glass bolted connection: the residual surface compression in the vicinity of the mounting hole, the localized stress concentration caused by drilling the mounting hole, and the hole-edge condition. This study is focused on developing an understanding of how the nominal residual surface compression affects the strength of glass around a mounting hole, for a given hole geometry and edge condition. For this reason, annealed, heat-strengthened, and tempered glass plates of identical geometry with centered mounting holes were tested, and ultimate loads were obtained for each specimen. By selecting glass specimens of identical geometry and hole diameter, the localized stress concentration around the mounting hole and the hole-edge condition were held constant. The nominal residual surface compression of each heat-treated glass specimens was measured using a GASP. FEA was utilized to calculate ultimate stress values based on the experimental ultimate loads. Ultimate stresses were then adjusted to generate strength values, expressed as equivalent 3-second load duration failure stress. Following this procedure, a direct relationship between glass ultimate strength and residual surface compression was established.

This section presented a detailed description of the problem considered in this thesis, and the research procedure devised to solve it. The following section offers a review of literature related to glass as a structural material. Previous research of residual surface compression in fully tempered glass with mounting holes, stress concentration

factors for plates with circular holes, and flaws caused by drilling of mounting holes in glass plates, is also presented.

3. LITERATURE REVIEW

Structural glass bolted connections are used to connect glass plates with pre-drilled mounting holes. Usually, the glass plates being connected are heat-treated glass plates (heat-strengthened or fully tempered). Based on existing knowledge related to annealed and heat-treated glass, it is believed that there are three factors which determine the strength of a glass bolted connection in the immediate vicinity of a mounting hole: the residual surface compression that originates from the heat-treatment process, the localized stress concentration caused by drilling the mounting hole, and the hole-edge surface flaws. This section aims to present relevant findings of previous research related to glass as a structural material, and the effects of the residual surface compression, localized stress concentrations, and mounting hole-edge surface condition to the strength of structural glass.

3.1. Glass as a Structural Material

Over the past few decades the use of glass as a structural material has increased significantly. Conventional windows, glazing of building facades, and internal building partitions are only a few applications of structural glass in the industry. Almost every type of flat glass in use today originates as annealed float glass, or simply annealed glass.

3.1.1. Annealed Float Glass

The manufacturing of annealed float glass starts with the continuous pouring of a molten mix of mostly sand, soda ash, and limestone onto a bath of molten tin. The mix of raw materials, having a higher melting point than tin, slowly solidifies while floating on

the molten tin. Thus, every glass plate produced through this method has a tin-side and an-air side. As the molten glass mix is slowly cooled to its final state, it creates what is referred to as annealed float glass, or annealed glass. Annealed glass is an isotropic linearly-elastic structural material (McLellan and Shand, 1984).

The manufacturing and handling process of a glass plate introduces flaws in its interior and surface. Furthermore, once placed into service, a glass plate is subjected to mechanical exposures and interactions that introduce additional flaws, as well as tensile stress fields in the surface of glass plates. The strength of annealed glass plates is controlled by the interaction between tensile stresses and stress-raising flaws (Beason, 1980; Beason and Morgan, 1984; Beason, et al, 1998). Stress raising flaws are interior or surface flaws that are located in the general area of a tensile stress field. Surface flaws usually play a greater role than internal flaws in the strength reduction of annealed glass because the magnitudes of tensile stress generated by common loading conditions are greater on the surface of a glass plate than in its interior, and because surface flaws tend to be more severe than internal flaws (Beason and Lingnell, 2000).

Since the introduction of annealed glass, the industry's demand for glass products that can withstand higher mechanical loads has evolved. Heat-treatment is a process that is used to enhance the strength and performance of annealed glass plates. The following paragraphs provide more information related to the heat-treatment of annealed glass.

3.1.2. Heat-Treated Glass

The strength of annealed glass plates is substantially increased by the heat-treatment process. During heat-treatment, annealed glass is heated near its softening temperature, and then quickly quenched. In the quenching process, the outer surfaces of

glass are air blasted and cooled at a faster rate than its interior. When the interior of glass eventually cools, a residual surface compression and an interior tensile stress distribution are locked into the glass. Figure 3 presents an idealization of the cross-sectional distribution of the residual surface compression through the thickness of heat- treated glass.

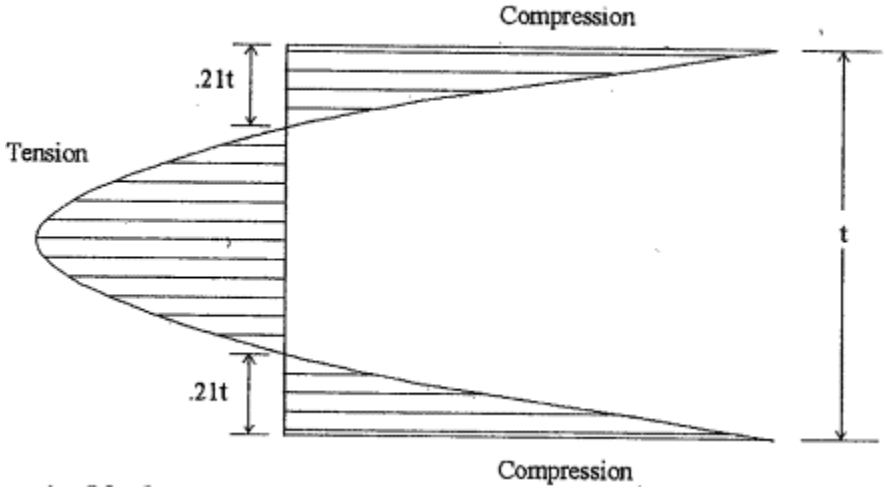

Figure 3. Idealization of the Residual Surface Compression in Heat-Treated Glass (reprinted from Beason and Lingnell, 2000)

The heat-treatment process is often controlled to develop two types of heat-treated glass: heat-strengthened and fully tempered glass (Beason and Lingnell, 2000). By definition, heat-strengthened glass is required to have a residual surface compression between 24 MPa (3,500 psi) and 52 MPa (7,500 psi), while tempered glass is required to have a minimum residual surface compression greater than 69 MPa (10,000 psi) (ASTM, 1997a). While heat-treatment significantly improves the strength of annealed glass, it

does not change the elastic properties of glass (Beason and Lingnell, 2000). In other words, heat-treated glass still remains an isotropic linearly-elastic material.

The following subsections present results from various experiments that have evaluated the effects of the residual surface compression in the immediate vicinity of a mounting hole, the localized stress concentration caused by drilling a mounting hole, and the hole-edge condition to the strength of structural glass bolted connections.

3.2. Study Conducted by Nielsen, et al.

This section provides information related to residual surface compressive stresses in the immediate vicinity of a mounting hole, and their effects on the apparent strength of structural glass bolted connections.

In 2009, Nielsen, Olesen, Poulsen, and Stang conducted a parametric study of residual stresses at holes in tempered glass (Nielsen, et al., 2009). The objective of the study was to evaluate the influence of residual compressive stresses at holes in tempered glass. FEA was used to simulate residual stresses as a variation of glass plate thickness, hole location and diameter, cooling rate, and far-field stress.

Nielsen, et al. described the strength of a tempered glass plate according to the following equation:

$$f_{TG} = \left|\sigma_{surf}\right| + f_{AG} \tag{3-1}$$

Where f_{TG} represent the strength of tempered glass, $|\sigma_{surf}|$ the residual surface compression, and f_{AG} the strength of annealed glass. Equation 3-1 quantifies a concept that has traditionally been used by engineers for the design of window glass.

Based on this assumption, and by utilizing Narayanaswamy's model of the tempering process (Narayanaswamy, 1971) on a FEA 3D model simulation, Nielsen, et al., were able to generate residual surface compressive stresses for different glass plate geometries with mounting holes. Of interest was the geometry presented in Figure 4.

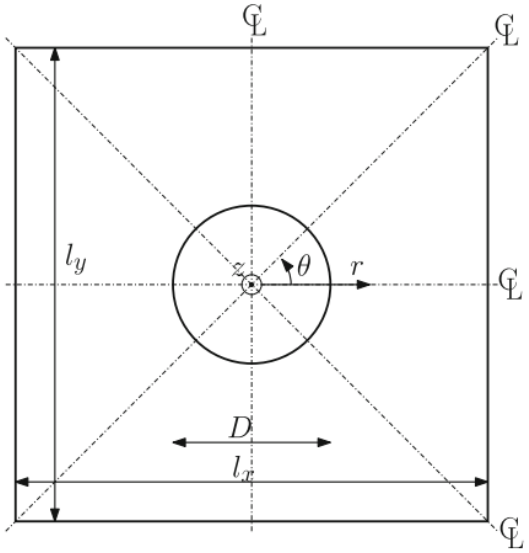

Figure 4. Sketch of Glass Plate with Centered Hole (reprinted from Nielsen, et al., 2009)

This study recognizes that the in-plane residual stresses around the mounting hole differ from residual stresses measured away from the mounting hole. Figure 5 presents the relationship between the critical value of in-plane residual stress around the mounting hole, σ_{rc}^{min}, and the residual stresses measured in the far-field, σ_{∞}, for a mounting hole located far from the edge of the plate, close to the corner of the plate, and close to the edge of the plate. These results were generated for a 500 x 500 x 19 mm plate (~19-11/16

x 19-11/16 x ¾ inch) with a 30 mm (~1-3/16 inch) diameter hole, and with a far field stress, σ_∞, of 83 MPa (12,038 psi).

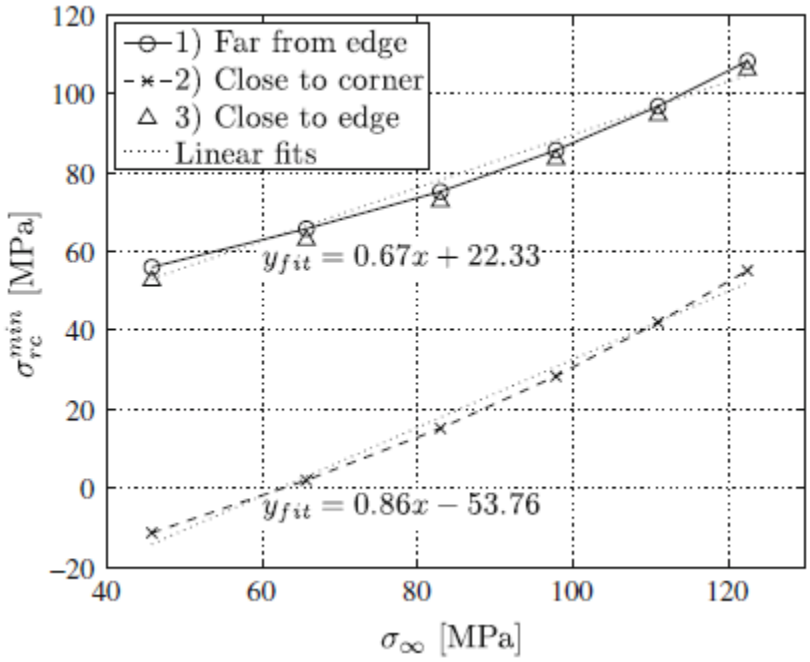

Figure 5. Far Field Stress vs Hole Residual Stress Correlation (reprinted from Nielsen, et al., 2009)

Through the use of FEA, simulations for different plate planar dimensions and hole diameters provide reliable estimations of the residual surface stresses in the immediate vicinity of a mounting hole. It was found that when considering larger plate planar dimensions, while maintaining the same 19 mm (~ ¾") thickness, the critical value of residual surface stress in the immediate vicinity of the mounting hole, σ_{rc}^{min}, converges to about 90% of the far-field stress, σ_∞ (Nielsen, et al., 2009). When considering glass

plates thinner than ¾", an increase in the critical value of residual surface stress in the immediate vicinity of the mounting hole was predicted using FEA (Nielsen, et al., 2009).

As stated above, the concept of Equation 3-1 is frequently used for the design of glass. Nielsen, et al. show that the presence of mounting holes in glass plates changes the distribution of the residual surface compression, $|\sigma_{surf}|$; specifically, the amount of residual stresses around the mounting hole differs from the residual stresses measured away from the mounting hole. In thinner glass plates such as those tested herein, Nielsen's results actually predict an increase in the localized residual surface compression in the vicinity of the hole. The purpose of this thesis is to develop an understanding of how the residual surface compression affects the strength of glass around a mounting hole, for a given hole geometry and edge condition. In other words, this thesis aims to verify that the concept expressed by Nielsen in Equation 3-1 is conservative for the design of structural glass bolted connections.

3.3. Studies Conducted by Peterson

This section presents literature findings that discuss the effects of localized stress concentration factors, which originate from the presence of a mounting hole, on the apparent strength of structural glass bolted connections.

Peterson's *Stress Concentration Factors* (Peterson, 1974) present a case study with similar support and loading conditions to the problem considered herein: stress concentration factors for bending of an infinite plate with a circular hole. The stress concentration factor *Kt,* vs hole diameter over plate thickness ratios are presented in Figure 6.

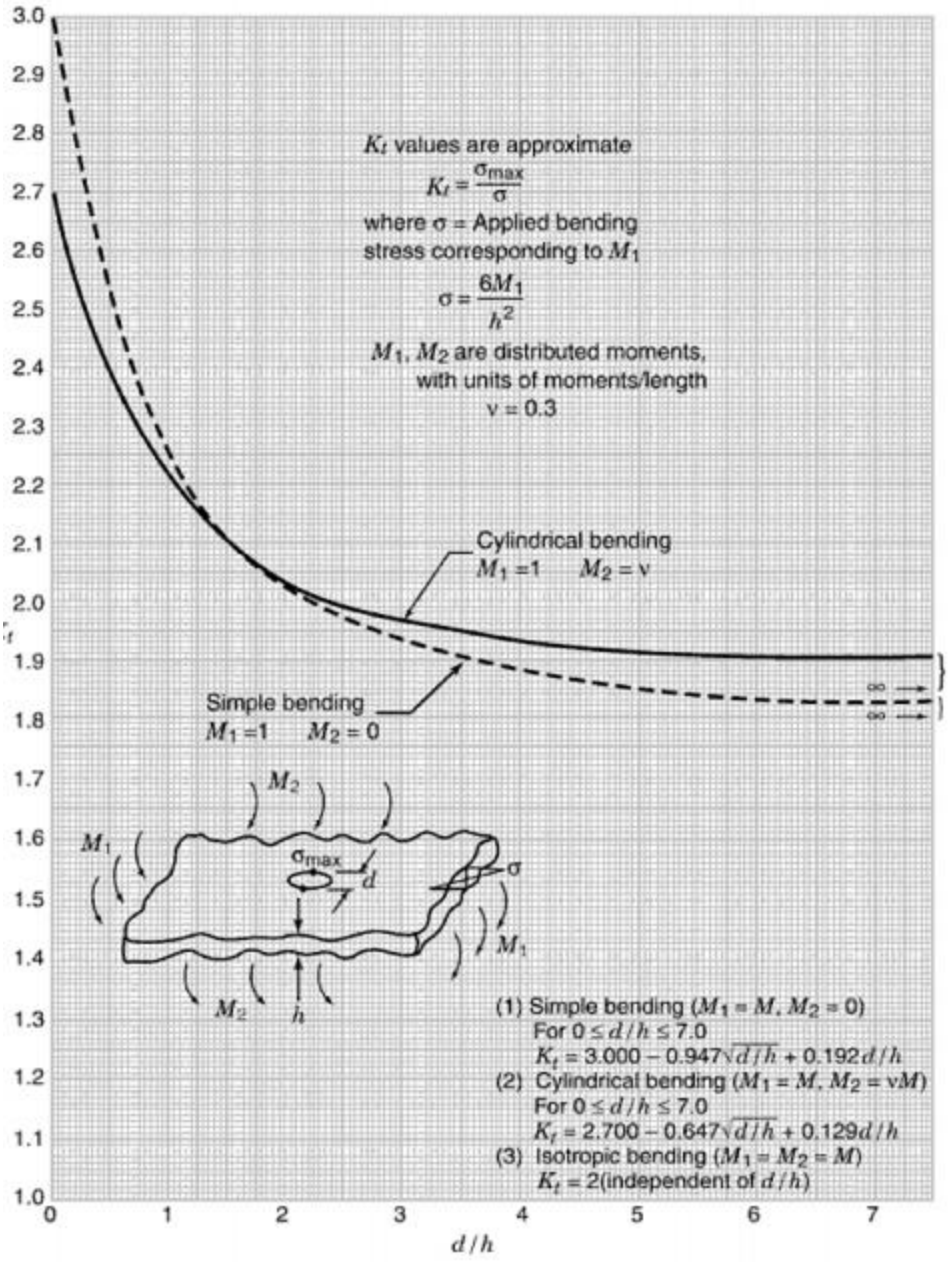

Figure 6. Stress Concentration Factors for Bending of an Infinite Plate with a Circular Hole (reprinted from Peterson, 1974)

The experiments conducted in this study consisted of glass plates with centered mounting holes, subjected to biaxial bending. Biaxial bending conditions are closest to

the isotropic bending shown in Figure 6, where $M_1 = M_2$. According to Peterson, the stress concentration factor, K_t, for isotropic bending of an infinite plate with a circular hole is:

$$K_t = 2 \quad (independent\ of\ {}^{d}/_{h}) \tag{3-2}$$

Where it is stated by Peterson that the stress concentration factor, K_t, is independent of the diameter of the hole, *d*, and the thickness of the plate, *h*. The loading and support conditions considered herein, while very similar to, they do not exactly match the conditions of bending of an infinite plate with a circular hole because the plates tested herein have finite in-plane dimensions. Alternatively, FEA techniques were used to model the exact loading and support conditions for the problem discussed herein and the calculated stress concentration factor was compared back to Peterson's case for infinite plates. The FEA estimation of the stress concentration factor applicable to this study is presented in the Evaluation of Results section.

3.4. Experiments Conducted by Lindqvist

The act of drilling a mounting hole in a glass plate introduces a population of flaws around the surface of the mounting hole-edge. This section presents previous research findings on the effects of these flaws on the strength of structural glass bolted connections.

In 2013, Lindqvist conducted experiments with the intention of predicting glass failure strength based on edge flaw characteristics (Lindqvist, 2013). Lindqvist aimed to

show that glass strength can be quantified in term of edge flaws. This research studied soda lime glass with edge flaws, which had originated during the manufacturing process.

In this research annealed glass specimens with five different edge finishes from various suppliers were investigated. Specimens were tested to failure using four-point bending to obtain strength values. The dimensions of manufacturing edge flaws on each specimen were measured using magnification techniques. These flaw dimensions were then paired to the experimental strength of each respective specimen.

Using fracture mechanics concepts, Lindqvist introduced a methodology that can be used to evaluate glass strength based on the dimensions of edge flaws. Of particular interest is Lindqvist's conclusion that the size of manufacturing edge flaws is one of the main factors that influences the edge strength of glass specimens (Lindqvist, 2013).

This literature review aimed to provide more information on previous research related to glass as a structural material, and the effects of the residual surface compression, localized stress concentrations, and mounting hole surface flaws to the strength of structural glass bolted connections. It shall be mentioned that while these three factors have been extensively studied, to the author's best knowledge, there has not been a study that considers the combined effects of these three factors on the strength of structural glass bolted connections.

4. EXPERIMENTAL EFFORT

Research discussed in the literature review indicates that the strength of structural glass bolted connections is directly influenced by the residual surface compression in the vicinity of the mounting hole, the localized stress concentration caused by drilling the mounting hole, and the hole-edge condition. This study is focused on the effects that the residual surface compression has on the strength of glass around a mounting hole, for a given hole geometry and edge condition. In essence, this thesis aims to determine if the concept expressed in Equation 3-1, presented by Nielsen, et al., is conservative for the design of structural glass bolted connections. For that purpose, glass specimens with varying levels of residual surface compression, and a given mounting hole geometry and edge condition, were tested. This section presents the experimental procedure that was followed to test the specimens.

4.1. Experimental Procedure

The purpose of this experiment was to obtain glass specimen measurements of residual surface compression and ultimate stress. This way, conclusions regarding the conservatism of Equation 3-1 for the design of structural glass bolted connections could be made. To calculate specimen ultimate stress values, specimen ultimate loads were entered into FEA models. Specimen ultimate loads, as well as residual surface compressive stresses, were determined following the experimental procedure described herein.

The experimental procedure was comprised of several steps. The first step was the selection and processing of glass test specimens. That was followed by the design of a

loading method and test machine that would subject the glass test specimens to biaxial bending. The last step of the experimental procedure was the recording of specimen ultimate loads. The following subsections expand on the mechanisms used to materialize the steps of this experimental procedure.

4.2. Test Specimen Selection and Processing

4.2.1. Test Specimen Selection

The selection of test specimens was an important step of the experimental procedure. Previous research conducted in the field of structural glass indicate that the strength of a structural glass bolted connection is determined by the residual surface compression in the vicinity of the mounting hole, the localized stress concentration, and the hole-edge condition. This study aims to better understand the effects of the residual surface compression on the strength of a structural glass bolted connection. To achieve that, the test specimens had to be selected based on a set of dimensional requirements, which are further explained in the following paragraphs.

In this experiment, annealed, heat-strengthened, and fully tempered glass plates were ordered. These specimens were subjected to a unique loading condition (Figure 2) that induces a uniform biaxial stress at the center of the plate. Test specimens were fabricated with ¼ inch glass that had planar dimensions of 16 x 16 inch. Each specimen had a drilled 1-7/16 inch diameter centered mounting hole, as shown in Figure 7. Following a statistical analysis for the number of glass plates to be tested in this experiment, 19 annealed, 21 heat-strengthened, and 21 fully tempered glass specimens

were tested. Table 1 provides a summary of the number of test specimens tested for each glass type.

Table 1. Glass Test Specimen Count

	Annealed	Heat-Strengthened	Fully Tempered
Specimen Count	19	21	21

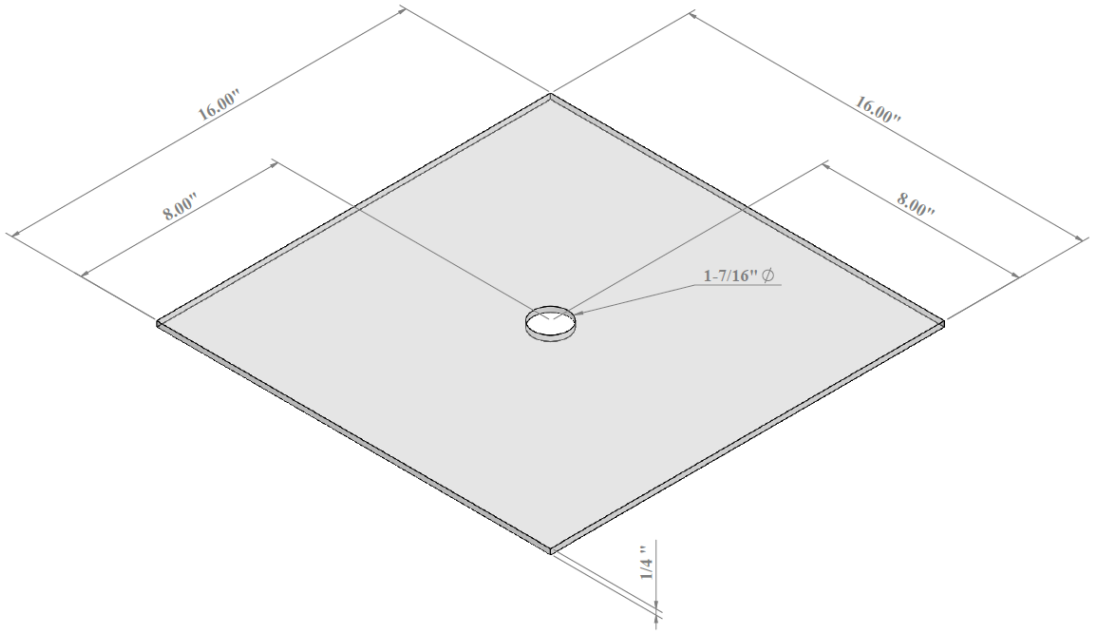

Figure 7. Isometric View of a Typical Glass Specimen

Structural glass bolted connections are comprised of a stainless-steel spider fitting that attaches glass plates to a supporting system. The spider fitting connects to the glass using a bolt that passes through a padded glass mounting hole. As indicated in Figure 1,

most spider fittings are manufactured with four legs, with the intention to connect four glass plates at one location. Thus, a typical glass plate that is part of a curtain wall system connected through spider fittings, has at least four mounting holes – one at each corner of the plate. Sometimes the plates have additional support points for larger plates. In the test procedure used in this thesis, a glass plate was subjected to biaxial bending in such a way that the maximum tensile stress occurred at the center of the plate. Therefore, a representative mounting hole was placed in the center of each specimen at the location of maximum tensile stress. Following the industry standards, the diameter of the mounting hole was to be no less than ¼ inches, and no greater than 16/3 inches (ASTM-C1048, 2012; Syracuse Glass Company, 2017). Consultation with industry experts led to the selection of a representative mounting hole diameter of 1-7/16 inch for this experiment.

As stated previously, the planar dimensions of the glass plates were 16x16 inches. There were several factors that dictated these dimensions. One factor was the stress concentration caused by the presence of a centered mounting hole in each glass specimen. It is generally believed that the effects of a mounting hole in the stress distribution of a rectangular plate offset at a distance of 5 – hole diameters away from the mounting hole. That coincides with a distance of about 8 inches away from the mounting hole, for the given hole diameter. Therefore, having glass plates with overall dimensions of 16x16 inches or greater should cause the strength of the plate to be closely approximated using Peterson's stress concentration factor for infinite plates; thus providing additional support for the stresses calculated using FEA. Therefore, it was determined that the planar dimensions of the glass plate specimens had to be at least 16x16 inches.

16x16 inch glass plate specimens proved to be easy to handle during transportation and testing. It is also reasonable to believe that the larger the size of a glass plate, the greater are the possibilities of inducing surface flaws to the specimen during the test setup. Another advantage to selecting glass plates with 16x16 inch planar dimensions was that symmetrical geometry of the plates allowed for a reduction of FEA modeling efforts and simulation time, as described later in this thesis.

All the glass specimens were ¼ inch thick. The ¼ inch dimension was a nominal one, and according to ASTM, manufactured glass plates shall have a minimum true thickness of 0.219 inch to be classified as ¼ inch glass. For this reason, measurements of each specimen's thickness were taken according to the procedure indicated in the test setup section. Test specimen thicknesses are shown in Appendix D.

As stated in the earlier paragraphs, this study aims to further understand the effects that the residual surface compression on the strength of glass in the immediate vicinity of a mounting hole. Because annealed glass has negligible levels of residual surface compression, while heat-strengthened, and fully tempered glass have to have minimal residual surface compression of 24 MPa (3,500 psi) and 69 MPa (10,000 psi), respectively (ASTM, 1997a), the effects of the mounting hole residual surface compression on the strength of a bolted connection can be better evaluated by testing identical annealed, heat-strengthened, and fully tempered glass plate specimens with centered mounting holes.

Lastly, the selection of glass plate specimens with identical geometry and mounting hole was done to keep the stress concentration and mounting hole edge-condition constant throughout this study. In the literature review, Peterson's conclusions

on stress concentration factors in rectangular plates with circular holes, indicate that the stress concentration factors depend strictly on the diameter of the hole, and geometry, loading and support conditions of the plate. Thus, by testing identical specimens under the same loading and support conditions, the resulting stress concentration factors remain constant, and are independent of the material properties of the tested specimen (Peterson, 1974).

It is believed that any random severe flaws induced around the surface of a mounting hole during the drilling process would cause the annealed glass plate to break when subjected to quenching. Therefore, it is likely that the hole-edge flaws that survived the heat treatment process would be less severe than the flaws associated with the original annealed specimens. This effect has the potential to make population of hole-edge flaw for annealed glass more severe on average than the population of hole-edge flaws for heat-treated glass because of the more severe hole-edge flaws would not survive the heat-treatment process. However, in this experiment, all test specimens, with the exception of two annealed glass plates that were excluded for particularly severe damage, appeared to have practically identical hole-edge surface conditions.

4.2.2. Test Specimen Processing

In this experiment, annealed, heat-strengthened, and fully tempered glass plates were subjected to biaxial bending. Test specimens were rectangular glass plates with planar dimensions of 16 x 16 inch and ¼ inch uniform thickness. Each specimen had a drilled 1-7/16 inch diameter centered mounting hole. Once obtained, specimens were prepared for testing. The preparation of a glass plate specimen for testing consisted of the initial inspection of the specimen for surface flaw condition, verification of specimen

dimensions, identification of the tin-side of the plate, measurement of nominal residual surface compression, and taping and labeling of the air side of the plate.

Test specimens were inspected for surface flaws. Special consideration was given to identifying flaws in the immediate vicinity of the mounting hole, also referred in this thesis as hole-edge surface flaws, or hole-edge condition. Records of this initial inspection were gathered for each specimen.

Following that, each specimen's thickness was measured. The thickness of each plate was obtained using a Mitutoyo IP65 micrometer, capable of producing thickness readings within 0.00005" accuracy (Mitutoyo, 2008). Figure 8 captures the micrometer measuring the thickness of a specimen. To assure that specimens had uniform thickness, micrometer readings were taken at different locations on a given specimen. The 16x16 inch planar dimensions of the glass plates, the centered position of the mounting hole, and the mounting hole diameter were also verified.

Figure 8. Micrometer Measurement of Specimen Thickness

The next step of the test specimen processing was the identification of the tin-side of the glass plate. During the earlier stages of the production of annealed glass, the molten glass mixture floats in a bath of molten tin. Therefore, every glass plate produced with this method has a tin-side and an air-side. The tin-side of the test specimens was detected using an ultraviolet (UV) light. The UV light facing the tin-side appears cloudy, as shown in Figure 9 because the tin-side has a higher UV reflectance than the air-side. Identifying the tin-side of a specimen was important for several reasons, which are further emphasized in the following paragraphs.

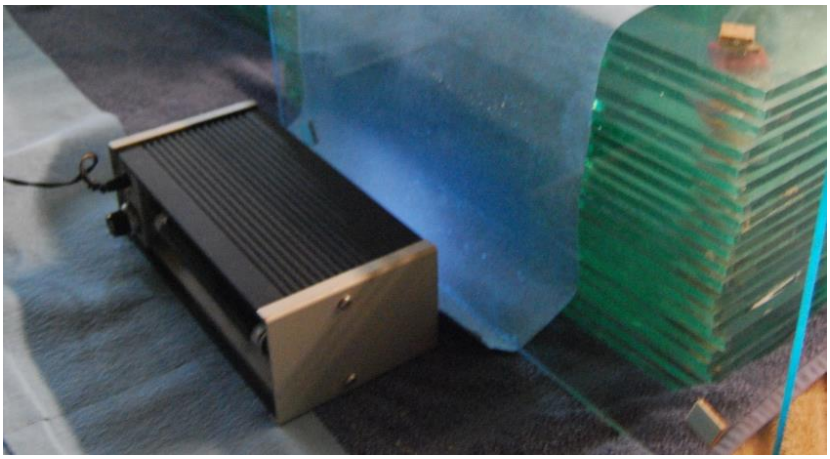

Figure 9. Cloudy Reflection of UV Light on Tin-Side

The nominal residual surface compression of each test specimen was measured using a Grazing Angle Surface Polarimeter (GASP) apparatus, shown in Figure 10. The GASP provided a conventional method to obtain quantitative, non-destructive measurements of residual surface compressive stresses (Strainoptics, 2017). More information about the technology and intended usage of the GASP can be found in the reference. To assure uniform levels of residual surface compression, GASP readings were taken at various locations away from the hole. The version of GASP used in this study could obtain residual surface compression readings only on the tin-side of the glass plates.

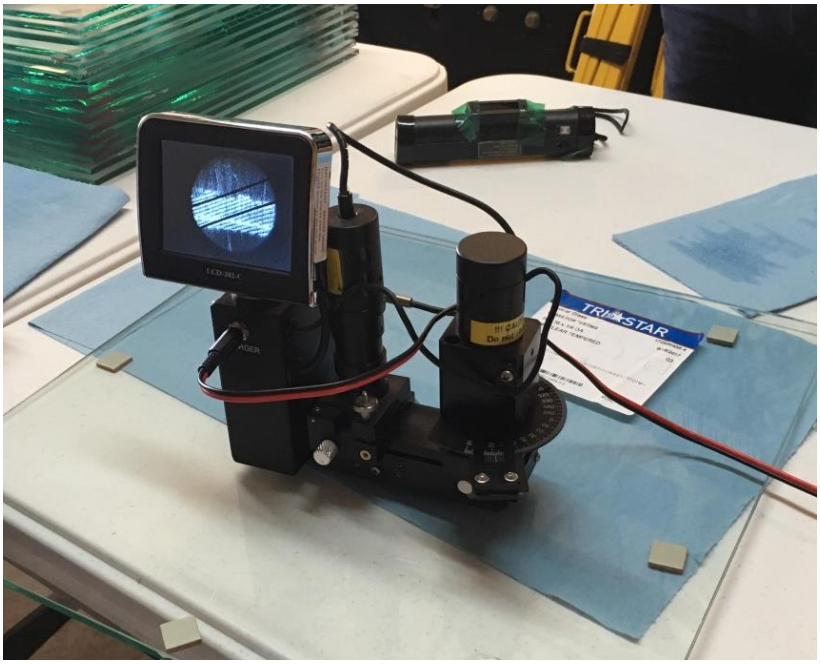

Figure 10. Grazing Angle Surface Polarimeter (GASP)

Because the strength of the tin-side of a glass plate is slightly lower than that of the air side at the time of manufacture (Sedlacek, 1999), bending glass specimens are often tested by applying the load to the air-side of the glass. Thus, the weaker tin-side of a glass plate sees the maximum tensile stresses induced from loading. In order to prevent the loss of fracture mirrors after the completion of the experiment, the air side of each glass plate specimens was taped. A fracture mirror is a small, relatively smooth circular or semi-circular surface, located near the fracture origin. The radius of the fracture mirror can be used as an alternative method to estimate the ultimate nominal stress of a specimen at the time of failure (Shand, 1959; Johnson and Holloway, 1966; Rodichev, et al., 2007).

After taping the air side of a given glass plate specimen, the flaw condition around the mounting hole was photographed. A photograph of a typical mounting hole

edge condition is shown in Figure 11. The documentation of the mounting hole edge condition was done at this stage of the test preparation, so that records of any additional surface flaws, which could possibly be induced during the test preparation process, were captured.

Figure 11. Photograph of a Typical Mounting Hole Edge Condition

After the inspection of all specimens for surface flaws, verification of specimen dimensions, identification of the tin-side of the plate, and measurement of nominal residual surface compression, specimens were labeled according to their glass type, and their air-side was taped. Throughout the years, this specimen preparation method has become standard for the testing of glass. A picture of a typical processed specimen prior to testing is shown in Figure 12.

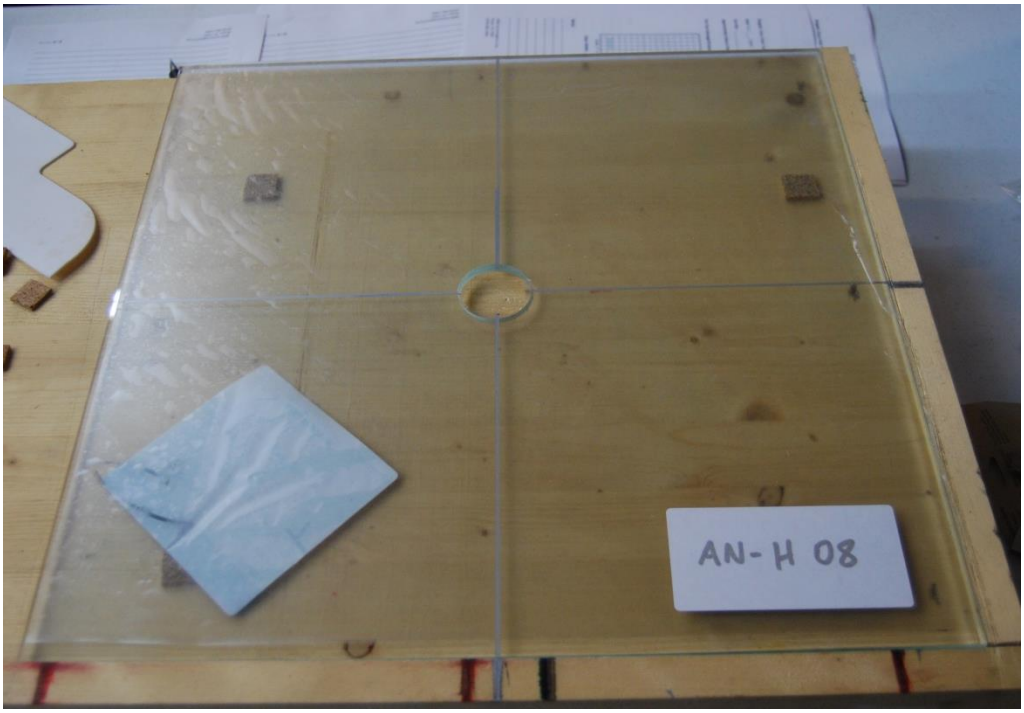

Figure 12. Glass Plate Specimen Prepared for Testing

Specimens were set up in the loading machine in a way that the loading and support conditions of the test would produce uniform ($\sigma_1 = \sigma_2$) biaxial bending stresses at the location of the mounting hole. More information about the loading method and procedure is provided in the following subsection.

4.3. Loading Procedure

4.3.1. Loading Method

When deciding a loading method that would adequately represent the loading and support conditions of window glass, consideration was given to three and four point bending, as well as biaxial bending (Figure 13). In comparing these loading methods, the

biaxial bending test appeared to have several advantages over the three and four point bending methods. A specimen subjected to biaxial bending experiences the same surface tensile in-plane stress in all directions. The center of the bottom surface of the specimen is in a tensile stress state (Torres et. al, 2014), and the volume of material under tension during biaxial bending is larger than that of the three and four point bending methods.

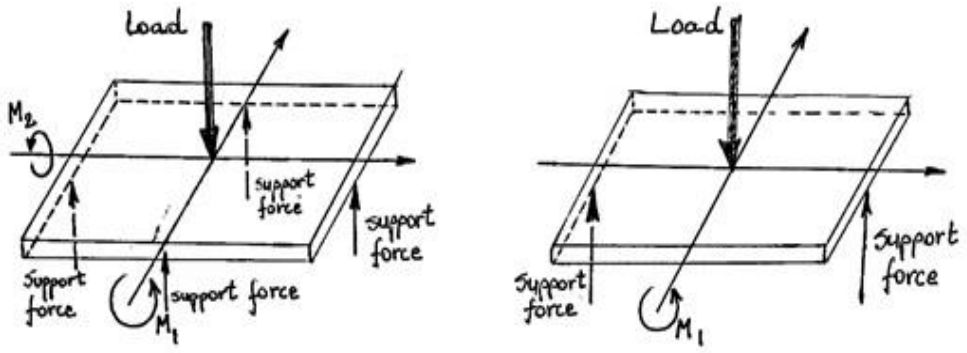

Figure 13. Schematic of Plate Biaxial Bending Test (Left) and Three Point Bending Test (Right)

Biaxial bending was also the testing method that most closely depicted the loading and support conditions of most window glass applications. However, when a glass plate is supported with spider fittings, the mounting holes are usually located at the corners of the glass plate. Yet, for such a connection, the maximum glass tensile stress under wind loads would still be located at the center of the plate. Furthermore, there are instances where glass plates are supported by a single fastener, going through a mounting hole located at the center of the plate. In any case, the loading and support conditions used in this experiment were designed to capture a "worst case" condition.

4.3.2. Loading Assembly

To ensure that the specimens were tested in biaxial bending, the structural support of the glass plates was designed as shown in Figure 14. Four rubber pads, placed at the center of each edge of a glass specimen, allowed for the bending of the plate in both major axes.

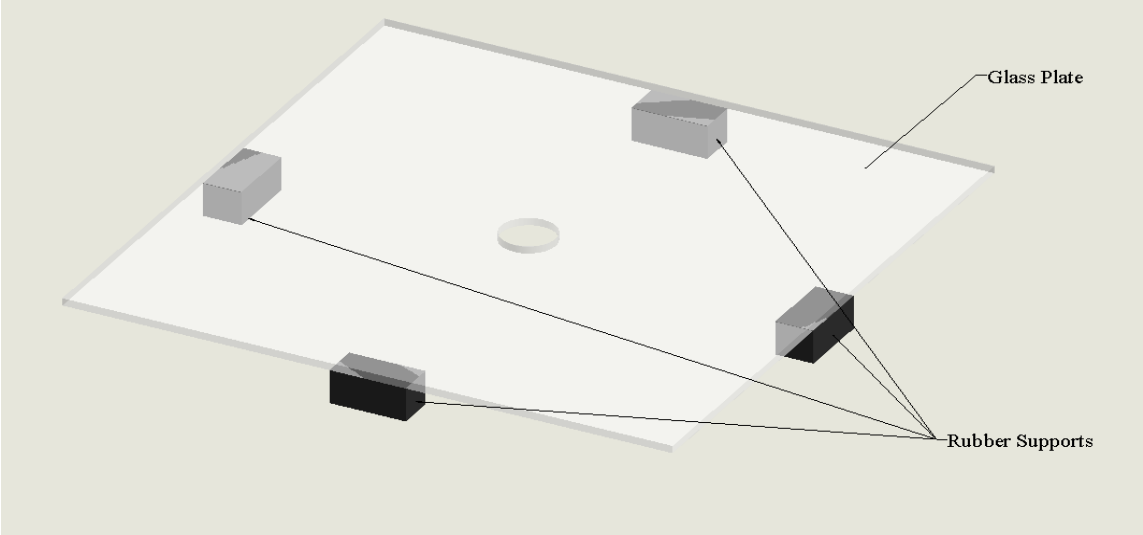

Figure 14. Drawing of Glass Plate Supports

A loading assembly was devised to apply a point load at the center of the glass plate specimens. The loading assembly contained a pneumatic cylinder, load cell, load spreading bar, electronic regulator, and a support platform. A schematic of the loading assembly is shown in Figure 15.

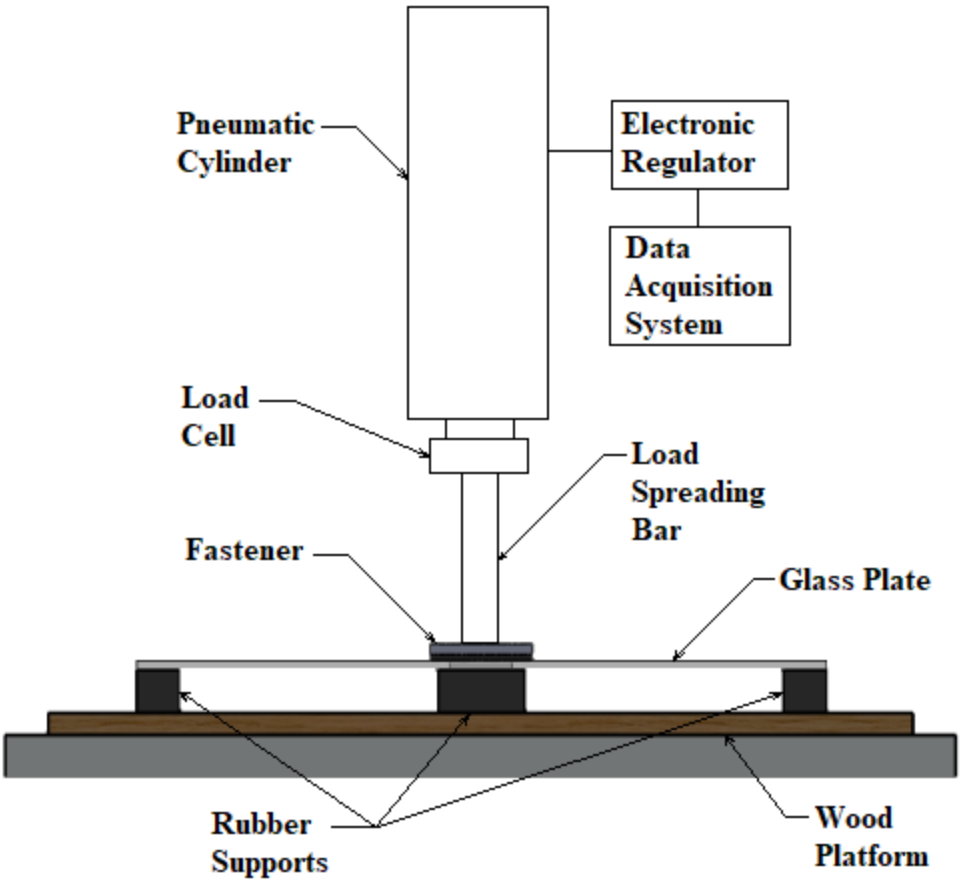

Figure 15. Schematic of Loading Assembly

Load was applied using a pneumatic (air) cylinder, capable of generating up to 1000 lb of concentrated point load. A load cell, installed as an extension to the pneumatic cylinder, recorded all the load values applied during the experiment. The load generated from the pneumatic cylinder, was transferred through a load spreading bar to a Brushed Stainless Heavy-Duty Exterior Swivel Fastener (HSFEX14BS). An image of a typical HSFEX14BS is presented in Figure 16. This type of fastener is adequate for a 1-7/16 inch diameter mounting hole, and can fit monolithic glass plates with a maximum thickness of 7/8 inches (CRL, 2010). During the experiment, only the fastener's interior load

spreading HDPE washer was in direct contact with the surface of the glass plate near the mounting hole. The HDPE washer had the shape of a ring with an inner diameter of ~ 1.362 inch, and an outer diameter of ~ 2.2885 inch.

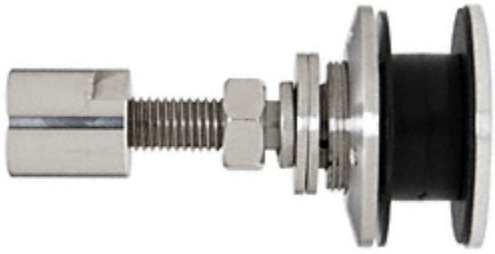

Figure 16. Typical HSFEX14BS Fitting (reprinted from CRL, 2010)

An electronic regulator unit was connected to the integrated load cell. Loading and data acquisition operations were controlled through the electronic regulator system. By programming a step function in the electronic regulator system, up to 650 lb of point load was applied by increasing the air cylinder pressure in increments of 0.5 psi per every 10 seconds (Figure 17). The 10 seconds time increment between each load step provided static loading characteristics, and minimized dynamic loading implications in the experiment.

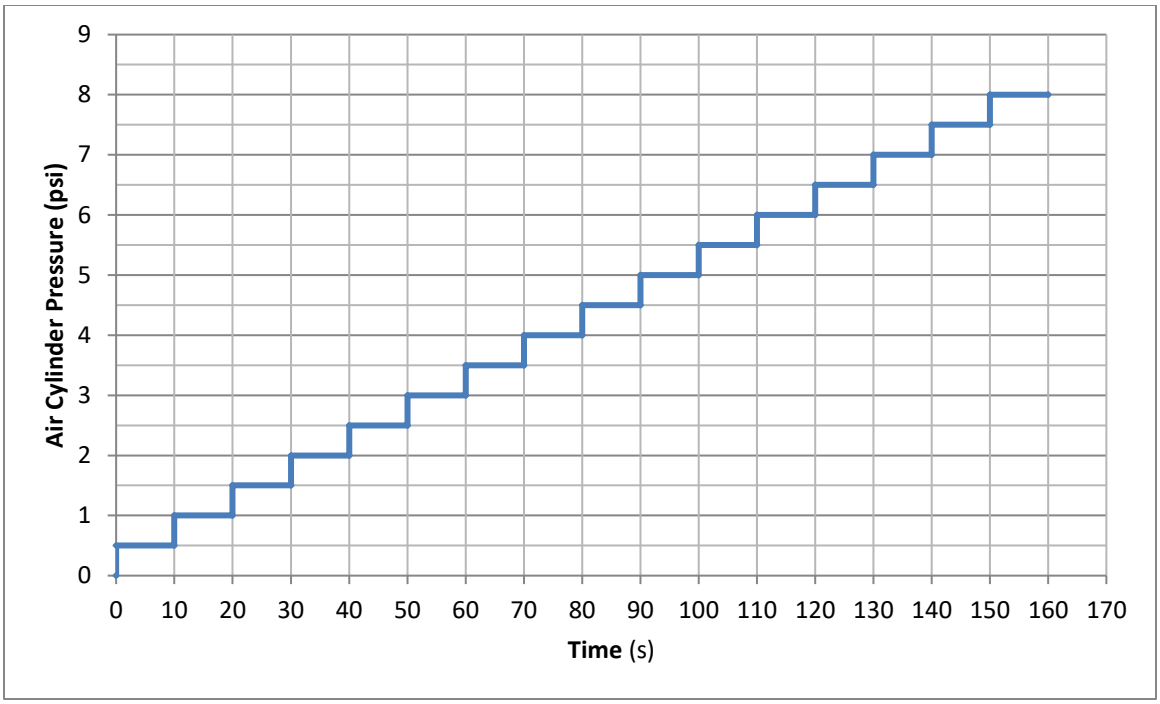

Figure 17. Graphical Representation of Air Cylinder Loading Function

Loading data were measured and recorded using the strain gauge load cell and the data acquisition system. At the time of testing indoor and outdoor environmental conditions were practically the same, with a recorded mean temperature of about 68°F and a mean relative humidity of 64. The ultimate failure loads, and other data gathered throughout this experiment, are shown in the following section.

4.4. Experimental Results

This section presents information gathered throughout the experimental procedure. First, GASP readings of nominal residual surface compressive stresses are shown in Table 2.

Table 2. Recorded Residual Surface Stress

Specimen Count	Annealed (psi)	Heat Strengthened (psi)	Fully Tempered (psi)
1	-	11014	13712
2	-	10160	14382
3	-	10160	15904
4	-	10160	15119
5	-	10160	15904
6	-	10160	15119
7	-	10160	15904
8	-	10160	15904
9	-	10160	15119
10	-	10574	15904
11	-	10160	15904
12	-	10160	15119
13	-	10160	15904
14	-	10160	15904
15	-	10160	15904
16	-	10160	15904
17	-	10160	15904
18	-	10160	15904
19	-	10160	15119
20	-	10160	15119
21	-	10160	15904

Following that, Table 3 presents the experimentally recorded specimen failure loads. A simple statistical analysis, the results of which are shown in Table 4, indicates that the failure loads of heat-strengthened glass specimens were very close to the failure loads of fully tempered glass specimens. This is related to the fact that heat-strengthened glass plates had very high values of residual surface compression. In fact, all of the specimens that were provided as heat-strengthened glass met the 10,000 psi limit for fully tempered glass and could be properly classified as tempered glass. However, this does

not present a problem because the residual surface compression for the tempered glass was also much higher than it had to be. In addition, the actual residual surface compression for each specimen was measured individually using GASP. So all inconsistencies were accounted for in the final analysis.

Table 3. Experimental Failure Loads

Specimen Count	Annealed (lb)	Heat Strengthened (lb)	Fully Tempered (lb)
1	155	480	521
2	155	521	562
3	155	480	562
4	114	521	521
5	155	521	562
6	155	480	521
7	155	562	521
8	114	439	521
9	155	439	562
10	155	521	562
11	155	480	521
12	155	439	521
13	155	439	562
14	155	439	521
15	155	480	562
16	155	521	562
17	155	439	521
18	155	439	562
19	114	439	562
20	-	521	521
21	-	480	602

Table 4. Statistical Analysis of Failure Load Data

	Annealed	Heat Strengthened	Fully Tempered
Mean (lb)	148	480	545
95% Mean CI Limits (lb)	141.1; 154.9	472.8; 487.2	542.8; 547.2
St Dev (lb)	15.3	39.1	24.3
COV (%)	10.35	8.15	4.46
St Dev of Mean (lb)	3.52	3.67	1.16

This section provided a description of the experimental effort of this thesis. An experimental procedure was established, and glass plate specimens were selected and processed for testing. A loading procedure that required the construction of a loading assembly, which would apply a biaxial bending stress to the test specimens, was designed. The loading assembly was also designed to electronically regulate and acquire experimental loading and deflection data. Values of residual surface compression measured by the GASP, along with experimental ultimate loads, were presented. These results are further discussed in the next section.

5. EVALUATION OF RESULTS

The focus of this thesis is to develop an understanding of how the residual surface compression affects the strength of glass around a mounting hole, for a given hole geometry and edge condition. In other words, this thesis aims to verify that the concept expressed in Equation 3-1 is conservative for the design of structural glass bolted connections. To achieve that, the experimentally recorded ultimate loads, presented in the previous section, were converted to ultimate stresses using the results of a geometrically nonlinear FEA. Standardized procedures, as presented by Beason and Morgan, were used to convert the calculated ultimate stresses to equivalent 3 second duration failure stresses (Beason and Morgan, 1984).

The following section describes in detail the FEA models used to convert ultimate loads to ultimate stress values, and the next section presents the conversion of ultimate stresses into equivalent 3 second duration failure stresses.

5.1. Finite Element Analysis

The purpose of this section is to develop a theoretical model that can relate the ultimate loads obtained during the experiment to their corresponding ultimate stresses. FEA models, matching the exact geometry and boundary conditions of the glass test specimens, were developed using ANSYS Parametric Design Language (APDL) 17.2. ANSYS is a commercial FEA software. Important components of the FEA models, such as element types, material properties, geometry, model discretization, boundary conditions, loading, results verification, and convergence study were implemented as

follows. Lastly, specimen ultimate stress values, which were estimated by entering experimental ultimate loads in the FEA models, were reported.

5.1.1. Element Selection

Selecting an appropriate element type is one of the most important steps of building an FEA model. ANSYS APDL has an extensive library of elements for FEA modeling. Each element type is specialized in modeling a specific range of physical problems. This range of physical problems depends on the number of nodes, and the types of numerical interpolation functions associated with a respective element. SHELL181, SOLID187, SOLID45, and SOLID186, found in the ANSYS Mechanical APDL Element Reference, were considered as possible model elements.

According to the ANSYS Mechanical APDL Element Reference, SHELL181 is suitable for analyzing thin to moderately-thick shell structures. This is a four-node element with six degrees of freedom at each node: translations in the x, y, and z directions, and rotations about the x, y, and z-axes (ANSYS, 2013). A geometrical representation of SHELL181 element is shown in Figure 18.

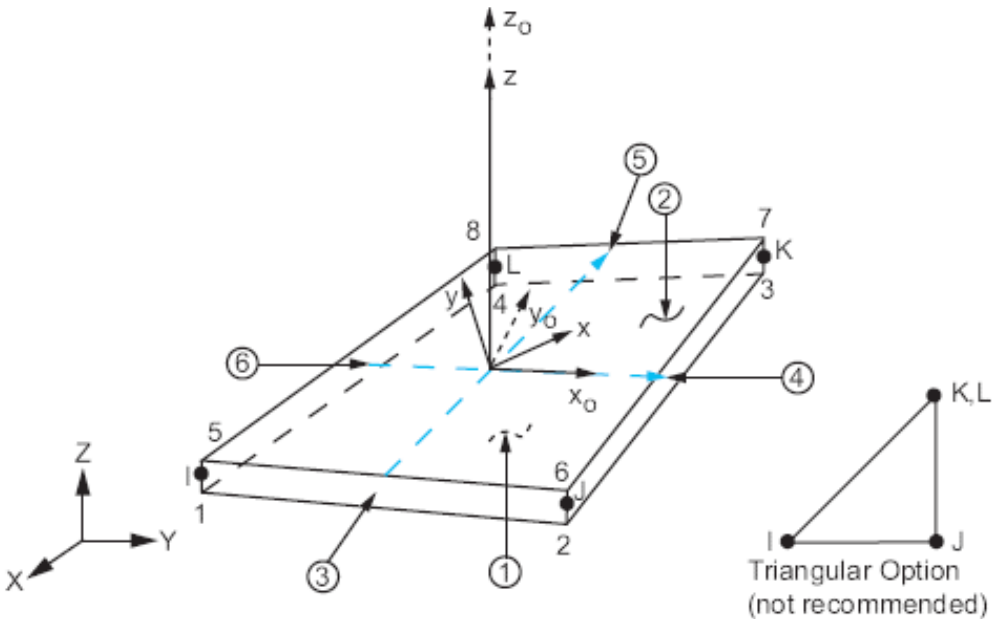

Figure 18. SHELL181 Geometry (reprinted from ANSYS, 2013)

Since the thickness of each glass specimen was approximately 1.5% of the specimen's length or width, the slenderness conditions to use shell elements were satisfied. SHELL 181 elements allow for a simplified 2D analysis of the problem at hand. Modeling the glass specimens with SHELL181 elements, consisting of only 4 nodes per element, can often reduce computational cost and modeling effort. Nevertheless, practical problems in structural glass design account for a variety of geometries and boundary conditions, which may not always be modeled well with shell elements. Furthermore, SHELL181 element thickness extends half of the thickness in each direction of its center plane, as shown in Figure 18. This would have made modeling of the connection between the rubber supports and shell elements very questionable. Therefore, SHELL181 elements, or any other shell elements, were ruled out.

SOLID187 element, shown in Figure 19, is a higher order 3-D, 10-node tetrahedral element. SOLID187 has a quadratic displacement behavior and is well suited to model irregular meshes. The element is defined by 10 nodes having three degrees of freedom at each node: translations in the nodal x, y, and z directions (ANSYS, 2013). In general, higher order elements yield results that are more accurate than their lower order counterparts (Wang, et al, 2004). Even through the quadratic interpolation functions often provide more accurate approximations of displacements than the linear interpolation functions of 8-noded elements, the wide range of numerical values between nodes that a quadratic function could theoretically achieve was cause for concern.

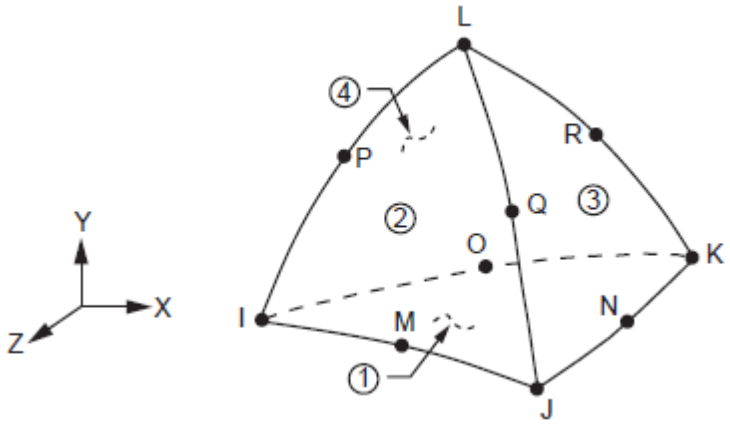

Figure 19. SOLID187 Geometry (reprinted from ANSYS, 2013)

To ensure proper modeling of the FEA problem, certain geometrical shapes of real elements had to be avoided. It is suggested that the interior angle at each vertex of an element should be in the range of 15°-165° (Reddy, 2006). Although this aspect of modeling is mainly related to the geometry mesh, there are situations that may force a violation of the angle range conditions mentioned above. In such situations, to prevent

numerical ill-conditioning of element matrices, it is suggested that the usage of SOLID187 element be avoided. Particular attention was also given to the stiffness variation of tetrahedral elements (Wang, et al, 2004). For the reasons mentioned, SOLID187 was not considered to be an effective modeling element for this experiment.

SOLID45 is an 8-noded brick element (Figure 20), used for the three-dimensional modeling of solid structures. Each node of the element has three degrees of freedom: translations in the nodal x, y, and z directions. Displacements and stresses in 8-noded brick elements are calculated at each node using linear interpolation functions (ANSYS, 2013).

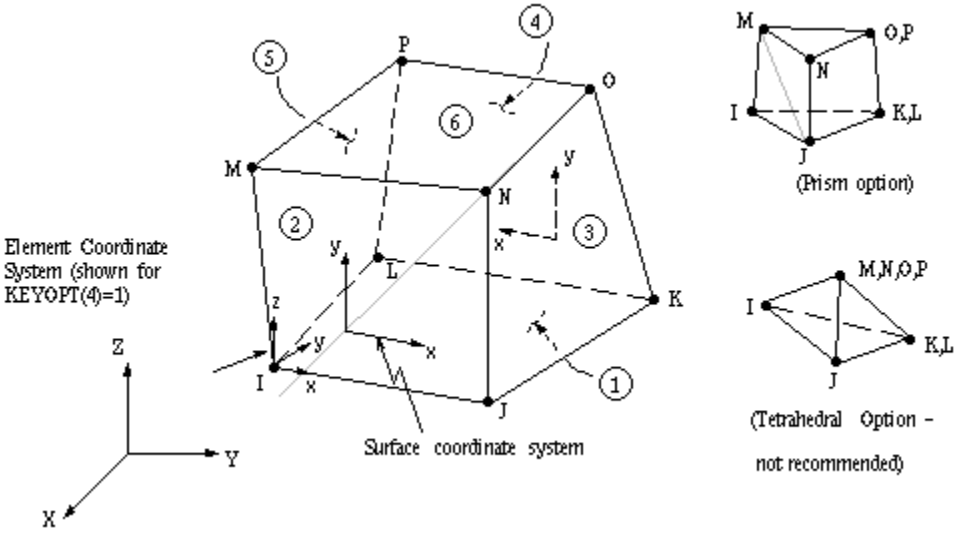

Figure 20. SOLID45 Geometry (reprinted from ANSYS, 2013)

By utilizing SOLID45 elements, the issues arising from using shell elements to model the connectivity between glass specimens and rubber supports could be avoided. Further, it is known that the displacement functions associated with linear elastic materials, such as

glass, are better modeled using 8-noded bricks than the quadratic SOLID 187 elements. Finally, these 8-noded brick elements easily comply with the regular mesh of the rectangular glass plates. Therefore, strong consideration was given to the application of SOLID45 elements in the FEA model of rectangular glass plates with mounting holes.

In this case, the areas around the hole were meshed manually with SOLID 45 brick elements, as shown in Figure 21. Detailed information about the meshing procedure of the FEA model is presented in the following subsections. Another point of concern was the transfer of stress through the thickness of the glass plate. For that reason, the glass plate specimens were modeled with a minimum of three elements through the thickness. Overall, SOLID45 was deemed to be an effective element for FEA modeling.

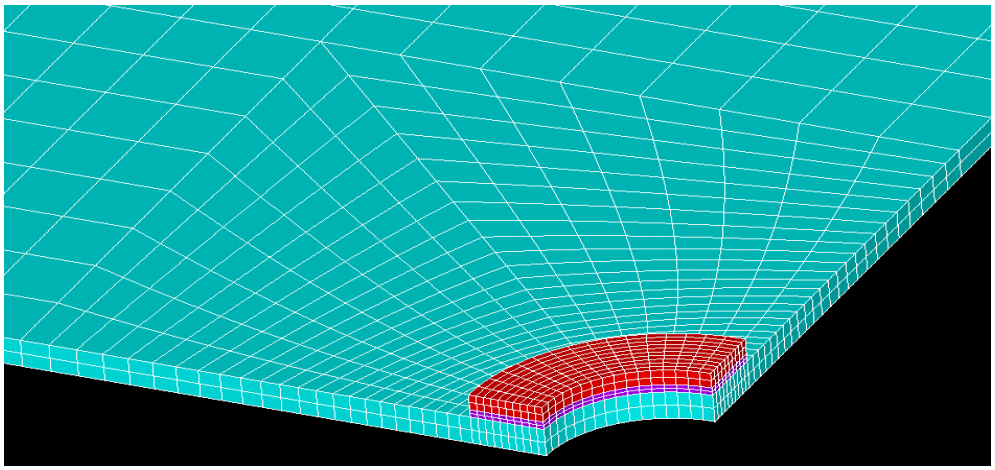

Figure 21. Brick Elements Used to Mesh a Circular Area

SOLID186 is a higher order 3-D 20-node solid element (Figure 22) that exhibits quadratic displacement behavior. The element is defined by 20 nodes having three

degrees of freedom per node: translations in the nodal x, y, and z directions (ANSYS, 2013).

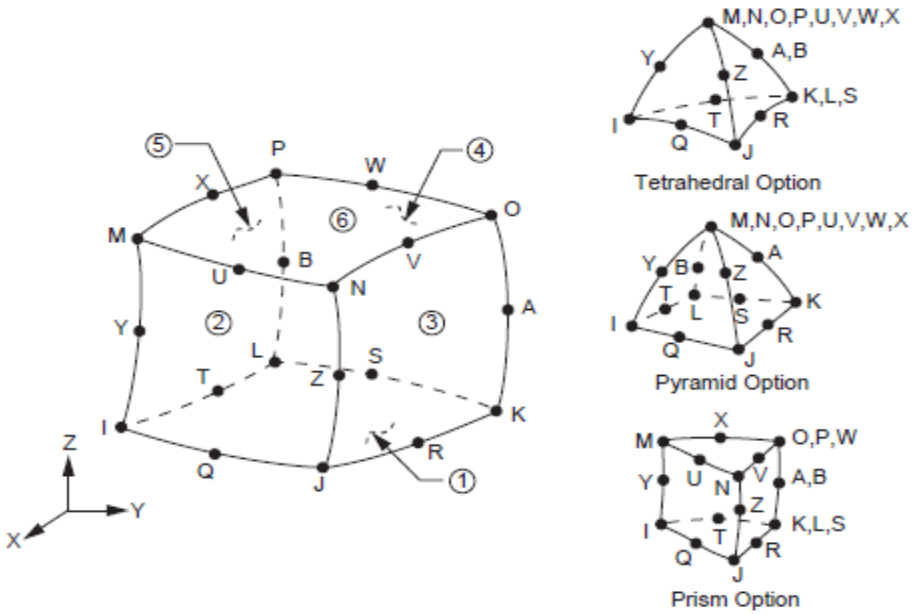

Figure 22. SOLID186 Geometry (reprinted from ANSYS, 2013)

Similarly to SOLID45, SOLID186 is an effective element for the FEA model of the glass plate specimens. However, the usage of SOLID186 instead of SOLID45 increased the computational time and cost of the FEA. Furthermore, SOLID186 elements also increased the uncertainty related to the wide range of numerical values between nodes that a quadratic interpolation function could theoretically obtain.

In conclusion, there were several elements that could have been utilized to generate the FEA model of the rectangular glass plates under biaxial bending. ANSYS element library provided readily available elements, such as: SHELL181, SOLID187, SOLID45, and SOLID186. While elements like SHELL181, SOLID187, and SOLID186

might produce accurate and reliable models for biaxial bending of rectangular plates, SOLID45 was selected to model the specific boundary conditions and geometry type of the problem considered herein.

5.1.2. Material Properties

As it can be noticed in Figure 23, at the time of testing, rectangular glass plate specimens rested on top of four rubber supports. The high-density polyethylene (HDPE) washer, which had an inner diameter of ~ 1-7/16 inch, an outer diameter of ~ 2-23/64 inch, and a 1/16-inch thickness, was in direct contact with the surface of the glass plate near the mounting hole. A 1/8-inch stainless steel plate, representing parts of the fastener, was modeled on top of the HDPE washer.

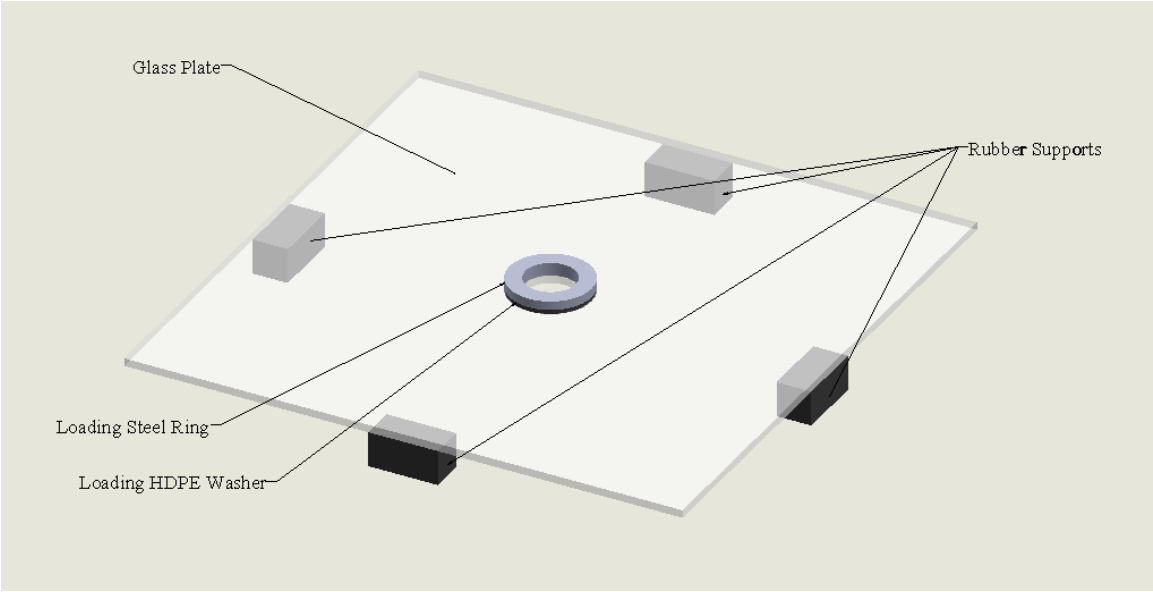

Figure 23. Sketch of Material Models for Finite Element Analysis

The material properties of the glass plate, rubber supports, HDPE washer, and stainless-steel ring were modeled in ANSYS Mechanical APDL 17.2. Since the elastic properties of glass remain unchanged until its failure point (McLellan and Shand, 1984; Beason and Lingnell, 2000), the glass specimen was modeled as a structural linear-elastic isotropic material. The Young's Modulus, E, and the Poisson's Ratio, υ, of glass were taken as 10.4E6 psi, and 0.22, respectively (McLellan and Shand, 1984). The rubber supports have a Young's Modulus of 2063 psi, and a Poisson's Ratio of 0.5 (AZoM, 2001).

Equation 5-3 relates a material's Young's Modulus, *E*, to its Shear Modulus, *G*, Bulk Modulus, *K*, and Poisson's Ratio, υ. While the Poisson's Ratio of rubber is about 0.5, a value of 0.499, was used instead, to avoid ill-conditioning of the FEA stiffness matrixes.

$$E = 2G(1 + \upsilon) = 3K(1 - 2\upsilon) \tag{5-3}$$

The stainless-steel ring was modeled with a Young's Modulus of 29E6 psi, and a Poisson's Ratio of 0.30 (ASM, 1990). The properties of each material utilized in the FEA model are summarized in Table 5. Given the application of the HDPE washer in the FEA models presented herein, HPDE was modeled as a structural linear-elastic material. An attempt to model HDPE as a nonlinear-elastic material produced the same results, while considerably increasing the computational time of the FEA model.

Figure 24 illustrates the path used to create a material model on ANSYS APDL 17.2. This procedure was followed to create the glass, rubber, HDPE, and steel material models.

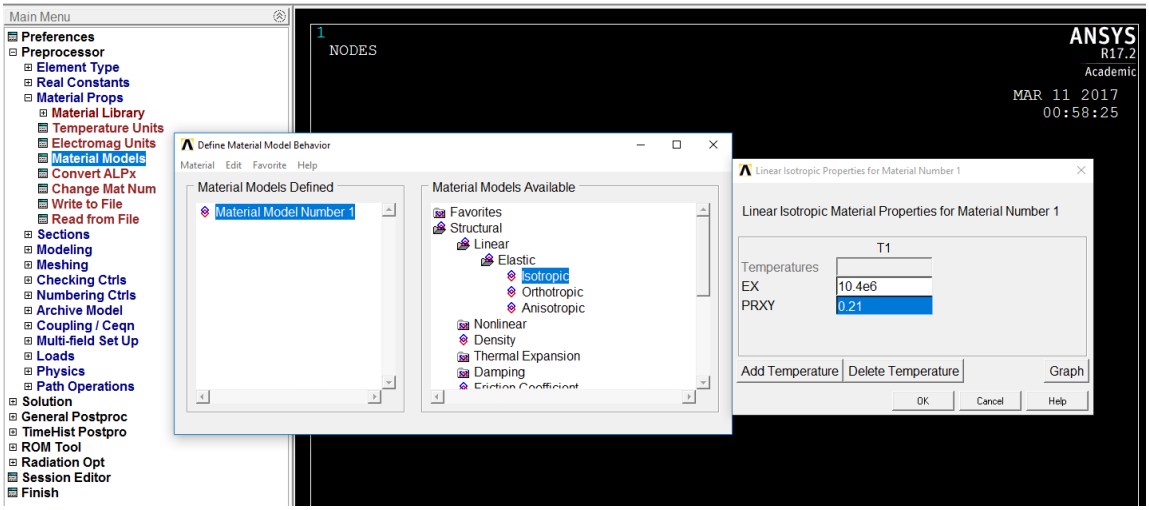

Figure 24. ANSYS Mechanical APDL Material Properties Entry Window

Table 5. Material Properties of the Finite Eelement Model

	Glass Plate	Rubber Support	HDPE Washer	Stainless Steel Ring
Young's Modulus *E* (psi)	10,400,000	2,063	134,450	29,000,000
Poisson's Ratio υ	0.220	0.499	0.450	0.300

5.1.3. Geometry Discretization

The division of the FEA model geometry into a number of subintervals/elements is referred to as the discretization of the FEA model. An FEA model is then solved

throughout each subinterval, providing for a versatile solution approach that can be implemented to the complex geometries of practical engineering problems (Reddy, 2006). This discretization was achieved by meshing the geometry of the model. As concluded in earlier paragraphs, elements were modeled as SOLID45 8-noded bricks. Therefore, the rectangular glass plates with centered mounting holes, rubber supports, HDPE washer and stainless-steel ring were meshed with 3D brick elements. To ensure proper meshing of the FEA model, attention was given to rules related to the geometrical shapes of elements. For instance, it is suggested that an element's length, width, and thickness are such that they do not surpass a ratio of 5:1 between each-other. Also, each face of a typical element shall have relatively smooth boundaries. For example, the interior angle at each vertex of an element should be in the range of 15°-165° (Reddy, 2006). Figure 25 shows a mesh of the rectangular glass plate with a mounting hole. Due to the symmetrical properties of the biaxial bending test, and the geometrical symmetry of the specimens, only a quarter of the plate was modeled for FEA.

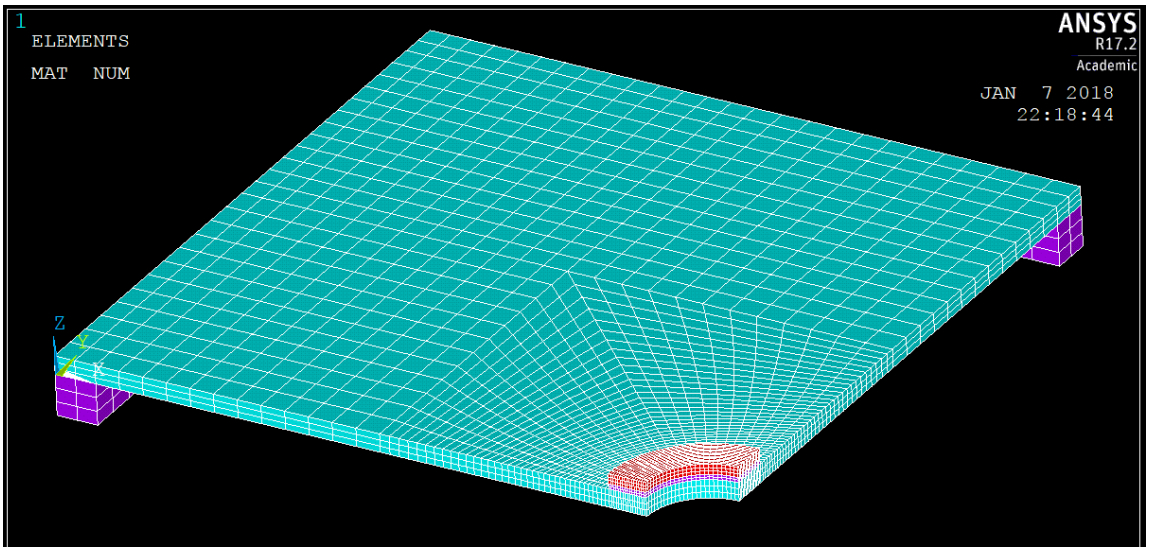

Figure 25. Mesh of Quarter-Model Specimen

The presence of the mounting hole required for the mesh of the glass plate to be non-uniform throughout the volume of the specimen. It is a common practice to refine a mesh by increasing the number of elements in the areas where the critical response, in this case 1st principal stress, is expected. Another reason for utilizing a non-uniform mesh is to ensure a proper modeling of the contact between the glass specimen and the rubber supports, and HDPE washer elements. ANSYS Mechanical APDL CONTACT elements are a readily available, straight-forward option for modeling of contact between different model components. The coefficients of friction used to model these contact elements are presented in Table 6.

Table 6. Friction Coefficients for Contact Element Models

	Rubber Support – Glass	HDPE Washer – Glass	Stainless Steel Ring – HDPE Washer
Coefficient of Friction, μ	0.220	0.45	0.300

Load was applied as a uniform pressure over the top area of the quarter-steel loading ring. This way, the FEA simulation closely emulated the conditions of the actual experiment. Additional information regarding symmetry boundary conditions, support boundary conditions, and load application is provided in the following section.

5.1.4. Boundary Conditions and Load Application

Essential boundary conditions (supports) were utilized to model the biaxial bending behavior of the glass specimens. Essential boundary conditions were satisfied by locking the Z-displacement at the bottom plane nodes of the rubber supports. Symmetry boundary conditions were applied to enforce the symmetrical behavior of the quarter-model. Furthermore, the symmetry boundary conditions assured that the plane sections remained plane throughout the thickness of the specimens. These boundary conditions were enforced by locking all the nodes of the right and left face of the model in the X and Y direction, respectively.

External forces, also referred to as natural boundary conditions, were applied as area pressures to the top surface of the stainless-steel ring. An illustration of the model boundary conditions and load application is presented in Figure 26. The theoretical model could relate the measured failure loads to ultimate stresses and maximum deflections in

each glass specimen. Thus, the FEA model was utilized to produce graphs that show load vs. stress, and load vs. deflection data. While load vs stress charts were the outcome of interest for this FEA study, load vs deflection charts were important to the verification of FEA results.

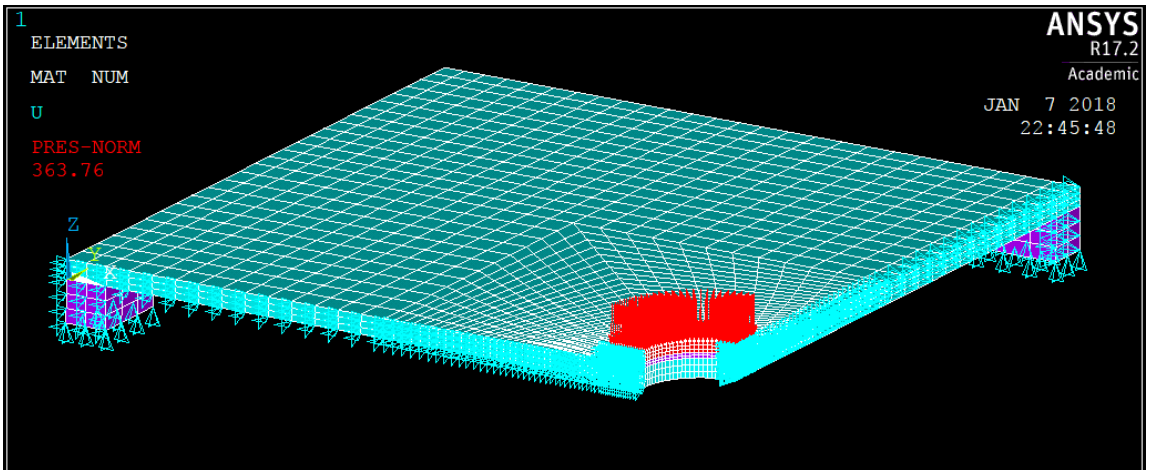

Figure 26. Boundary Conditions & Load Application for the Quarter-Plate Model

Table 7 presents the load values that were entered in the FEA model. Loads were inputted as pressures over the quarter-model stainless-steel ring area. The FEA simulation results obtained from these loads were recorded, and the respective load vs. stress, and load vs. deflection graphs are shown in later sections.

Table 7. Finite Element Model Applied Loads

Simulation #	Total Load Applied (lb)	Loading Ring Area (in^2)	Applied Pressure (psi)
1	100	2.92	**34.30**
2	200	2.92	**68.61**
3	300	2.92	**102.91**
4	400	2.92	**137.22**
5	500	2.92	**171.52**
6	600	2.92	**205.83**
7	700	2.92	**240.13**
8	800	2.92	**274.43**
9	900	2.92	**308.74**
10	1000	2.92	**343.04**
11	1100	2.92	**377.35**
12	1200	2.92	**411.65**
13	1300	2.92	**445.96**
14	1400	2.92	**480.26**
15	1500	2.92	**514.56**
16	1600	2.92	**548.87**
17	1700	2.92	**583.17**
18	1800	2.92	**617.48**
19	1900	2.92	**651.78**
20	2000	2.92	**686.09**

The following subsection describes the structural analysis method implemented to the FEA models. A special consideration was given to the geometric nonlinearity effects that are present in the analysis of members with large deflections.

5.1.5. Analysis Method

Prior to the point of failure, plates subjected to lateral loads generally experience deflections that may exceed at least half of their thickness. These relatively large

deflections may cause the middle plane of the glass plate to stretch, leading to an introduction of membrane stresses (Timošenko and Woinowsky-Krieger, 1959). Therefore, to capture the correct deflections and stress distribution of a glass specimen under lateral loads, the application of a geometrically nonlinear stress analysis is required (Vallabhan and Wang, 1981; Beason and Morgan, 1985; Beason and Norville, 1990). ANSYS Mechanical APDL allowed for the implementation of the geometric nonlinearity. Figure 27 indicates the *Solution Controls* window, under the *Solution* directory in ANSYS Mechanical APDL 17.2. Geometric nonlinearity was implemented in this analysis through the *Large Displacement Static* option under the *Analysis Options* tab. The number of sub-steps entries is left to the discretion of the user. For a given load magnitude, ANSYS will start the analysis by dividing the load into small portions. The number of these portions matches the number of sub-steps entered by the user. ANSYS solves the problem for the first sub-load, checks if the answers converge, and records the answers, which are then used as initial conditions for the following sub-load problem. When relatively large loads are inputted into a model, a large number of sub-step entries increase the possibility for a solution convergence to take place. A large number of sub-steps entries also increase FEA computational time and analysis cost. For the problem discussed herein, a number of 20 sub-steps was considered appropriate. If 20 sub-steps are not acceptable, the ANSYS analysis will automatically increase the number of sub-steps, until convergence is satisfactory.

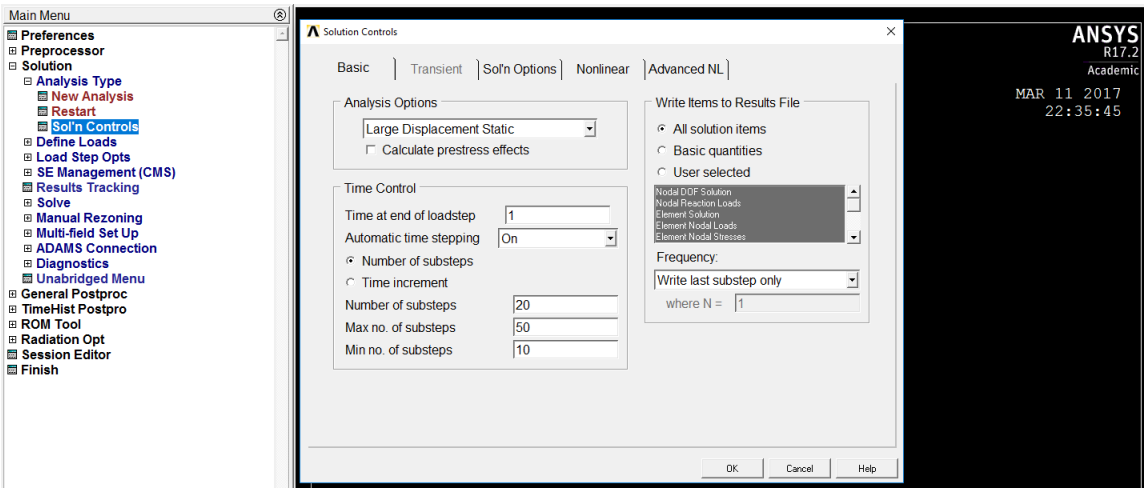

Figure 27. ANSYS Analysis Controls Window

Due to the many uncertainties that originate in the element selection, material property modeling, mesh pattern, boundary condition application, and analysis type of the FEA simulation, it is necessary to verify the accuracy and reliability of the FEA model results. The following subsection verifies the results of the finite element method by observing ANSYS solutions to structural benchmark problems.

5.1.6. Finite Element Analysis Results Verification

To verify the accuracy and reliability of the results produced by the FEA model, a series of benchmark problems are solved using ANSYS Mechanical APDL. A cantilever beam problem was the first benchmark problem considered. This problem was supposed to validate the capability of ANSYS in producing exact solutions, while implementing Euler-Bernoulli's small displacement theory. The next problem considered was a uniformly loaded, simply supported rectangular plate, the solution to which required the use of geometric nonlinearity. The last problem considered herein was the verification of

the Peterson's stress concentration factor of 2 for the biaxial bending of the glass plate test specimens with centered mounting holes.

A 12x4x1 glass cantilever beam was loaded on the top surface with a uniform area pressure, *w(z)*, of 1 psi. The beam maximum deflection was calculated to be 0.002991 inch, and the maximum bending stress, σ_{max}, experienced by the beam was found to be 432 psi using Euler-Bernoulli's small displacement theory. Detailed computations of the cantilever beam's maximum displacement and stress are shown in Appendix A.

It is important to understand that for a problem that can be correctly solved through the use of small deflections, a properly executed large deflection analysis should yield results that match its small deflection counterpart. The small deflection solution indicated a maximum displacement of 0.002966 inch, and a maximum 1st principal stress of 438.812 psi. Both of these calculated values were within 2% of their respective exact solution. Similarly, the large deflection solution provided a maximum deflection of 0.002966 inch, and a maximum 1st principal stress of 438.806 psi. The large deflection solutions also were within 2% of the analytical solutions. Table 8 presents a summary of the exact solution, and the FEA small and large deflection solutions.

Table 8. Summary of Cantilever Beam Problem Solution

	Exact Solution	FEA Small Displacement Solution	FEA Large Displacement Solution
Max Deflection (in)	0.002991	0.002966	0.002966
% Error	Datum (N/A)	0.84	0.84
Max Stress (psi)	432	438.812	438.806
% Error	Datum (N/A)	1.58	1.58

The next step in the verification of the FEA model generated by ANSYS, was the solution of a large deflection problem. The behavior of uniformly loaded rectangular plates has been examined by Timošenko in his *Theory of Plates and Shells* (Timošenko and Woinowsky-Krieger, 1959). Following that, other researchers have utilized computational tools to improve upon the analysis of rectangular glass plates (Beason, 1980; Vallabhan and Wang, 1981). Beason utilized ALGOR, another FEA software, to achieve results that matched his previously established solution to rectangular glass plates subjected to lateral uniformly distributed wind loads. Therefore, the second benchmark problem is related to the evaluation of maximum deflection and stress of a simply supported 60x60x1/4-inch glass plate under a lateral uniform area pressure of 0.50 psi. The modulus of elasticity of glass is 10.4 E6 psi, and its Poisson's ratio is 0.22.

Appendix B provides results from the respective ALGOR and ANSYS solutions to the maximum lateral displacement seen by the simply supported glass plate. Table 9 summarizes the stress and deflection results gathered from the ALGOR and ANSYS FEA model simulations. It can be noticed that the answers provided by ANSYS are within 1% of the already verified ALGOR results.

Table 9. Summary of Large Plate Problem Solution

	ALGOR Solution	ANSYS Solution
Max Deflection (in)	0.867538	0.867781
% Difference	Datum (N/A)	0.03
Max Stress (psi)	5674.81	5632.69
% Difference	Datum (N/A)	0.74

As indicated in the literature review, Peterson specified that the stress concentration factor applicable to the biaxial bending of an infinite plate with a circular hole was *Kt* = 2. To verify that the FEA model of the finite glass plate with a centered mounting hole incorporated a stress concentration factor of about 2, another FEA model of a glass plate without a mounting hole was created. Both models had identical planar dimensions, thicknesses, loading and support conditions. The FEA models were subjected to loads ranging from 100 lb to 2000 lb, with 100 lb increments. Values of deflection factor, R, and stress concentration factor, Kt, were calculated for each load-step, using the following:

$$R = \frac{\delta_H}{\delta_{NH}} \tag{5-4}$$

$$K_t = \frac{\sigma_H}{\sigma_{NH}} \tag{5-5}$$

Where δ_H is the maximum Z-deflection of the glass specimen with a mounting hole, δ_{NH} is the maximum Z-deflection of the glass specimen without a mounting hole, σ_H is the maximum 1st principal stress of the glass specimen with a mounting hole, and σ_{NH} is the maximum 1st principal stress of the glass specimen without a mounting hole. Values of deflection and stress concentration factors estimated through Equation (5-4) and (5-5) are shown in Table 15 of Appendix C.

It was found that the deflection of the rectangular glass plate with a hole was very similar to the deflection of the rectangular glass plate without a hole. It was also found

that the average stress concentration factor of the FEA model used in this study was roughly 2.0, which matched the stress concentration factor predicted by Peterson for an infinite glass plate with a centered hole (Peterson, 1974).

This section verified the FEA solution accuracy to a variety of structural benchmark problems. The FEA solution to a classic cantilever beam problem was considered. The solution to a simply supported rectangular plate subjected to uniform wind loads was achieved through the use of geometric nonlinearity. Furthermore, the stress concentration factor of the ANSYS FEA test specimen models was verified to match Peterson's stress concentration factor of 2. This factor is applicable to the biaxial bending of the glass plate test specimens with centered mounting holes. The following section presents a convergence study of the FEA model.

5.1.7. Convergence Study

To stabilize the results of the FEA model, a mesh convergence study was conducted. FEA models are meshed into a large number of elements with specific structural properties. These elements introduce points of interpolation for the eventual solution of the FEA model. Therefore, a finer model mesh constitutes of a larger number of elements, and thus, yields more accurate results than a coarser mesh. Yet, the larger number of elements requires a considerable amount of computational time and effort to produce a solution. A convergence study is the procedure of selecting the proper model discretization by considering the model solution accuracy and computational cost for different mesh densities.

Four model mesh patterns were examined as part of the convergence study. Each mesh pattern was designed to comply with established guidelines for mesh element

aspect ratios. One such guideline suggests that an adequate FEA model must have elements with a maximum dimensional aspect ratio of 5:1, combined with element interior angles in the range of 15°-165° (Reddy, 2006). Figure 28 - Figure 31 show isometric views of the four mesh types discussed herein.

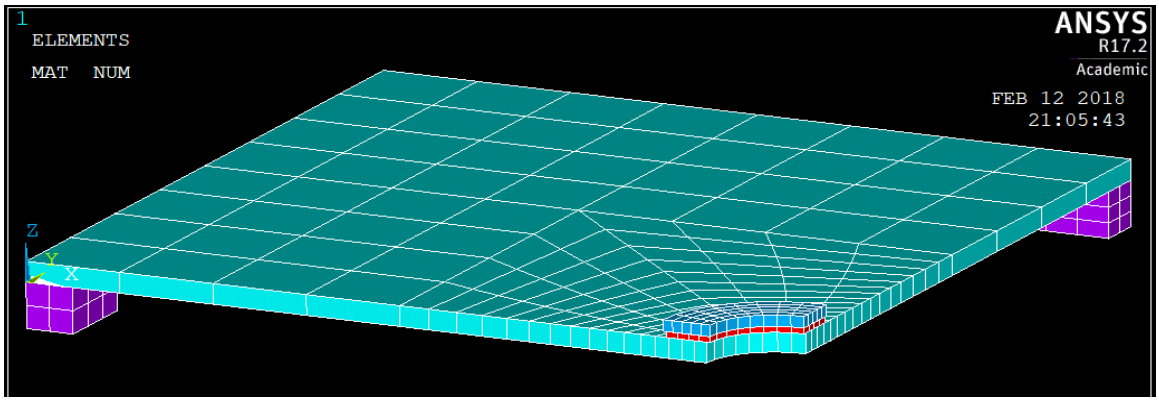

Figure 28. Mesh Type 1 - Isometric View of Model with 307 Elements

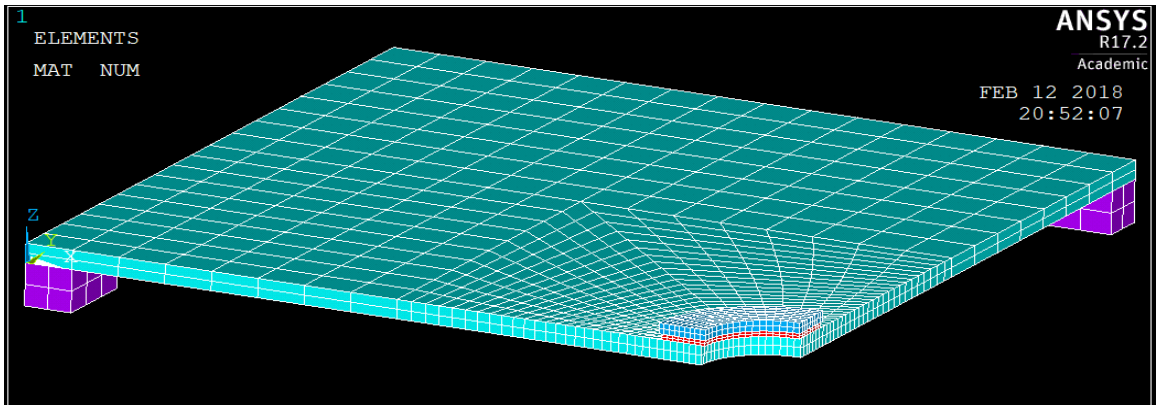

Figure 29. Mesh Type 2 - Isometric View of Model with 2,264 Elements

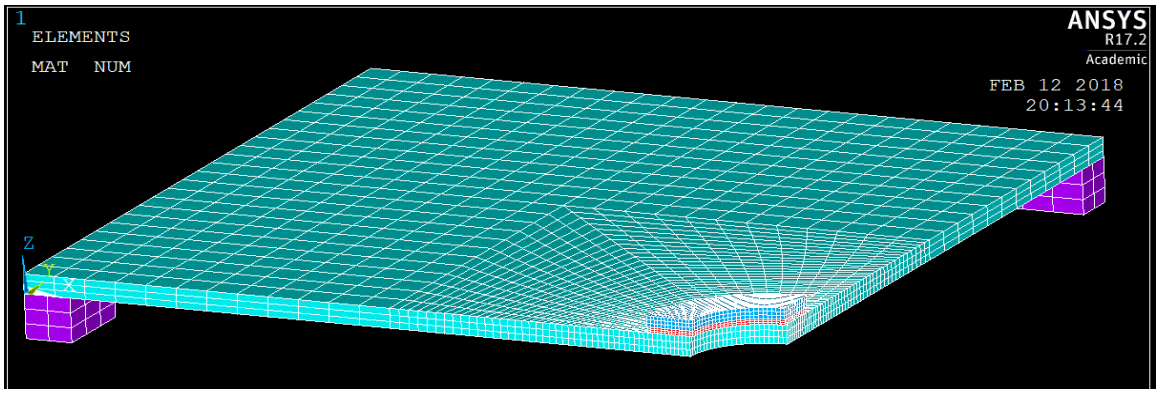

Figure 30. Mesh Type 3 - Isometric View of Model with 7,296 Elements

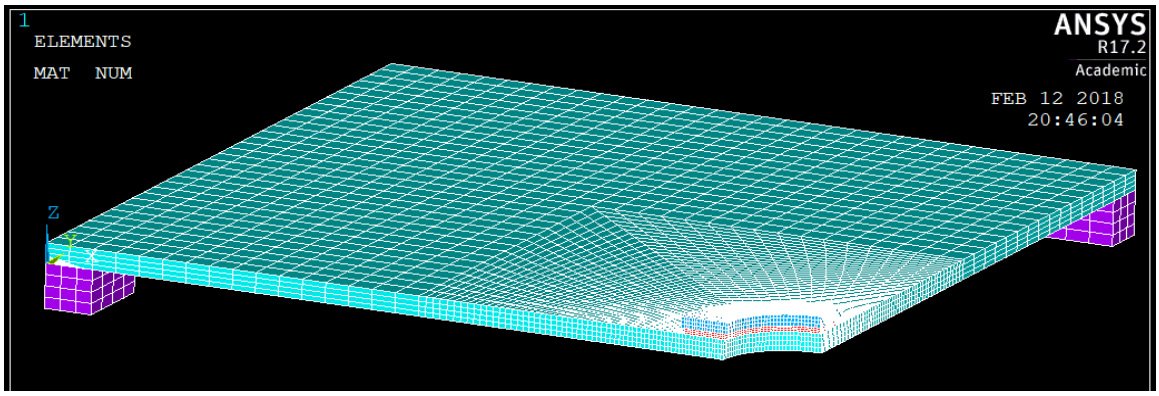

Figure 31. Mesh Type 4 - Isometric View of Model with 16,664 Elements

The main difference between these meshed models was the number of elements along the thickness of the glass plate. The mesh type number corresponded with the number of elements through the glass thickness; for example, mesh type 1 had one element through the thickness of the glass plate, while mesh type 3 had three such elements. Throughout this convergence study, several components of the FEA models were kept constant. All meshed models were subjected to an area pressure equivalent to a 1000 lb of total load. The area pressure was applied on the top surface of the stainless-

steel loading ring. The material properties of the glass specimen, rubber supports, HDPE washer and stainless-steel ring were also kept constant. Thus, the only variable of this study was the mesh density.

The maximum displacement in the downward Z-direction and the 1st maximum principal stress were recorded at the lower, bottom-right corner of the quarter plate model. The displacements and stresses for each mesh type are presented numerically in Table 10, and graphically in Figure 32 and Figure 33. In calculating the % difference between the results of each mesh type, the displacement and stress of the finer meshed model were used as datum.

Table 10. Model Convergence Study of Z-Displacement and Stress

Mesh Type #	Mesh Density	Z-Displacement (in)	% Difference	Stress (psi)	% Difference
1	307 Elements	0.285525	1.54	47,993.50	-3.35
2	2,264 Elements	0.288225	0.61	46,924.20	-1.05
3	7,296 Elements	0.291598	-0.56	46,616.90	-0.38
4	16,664 Elements	0.289985	0.00	46,438.30	0.00

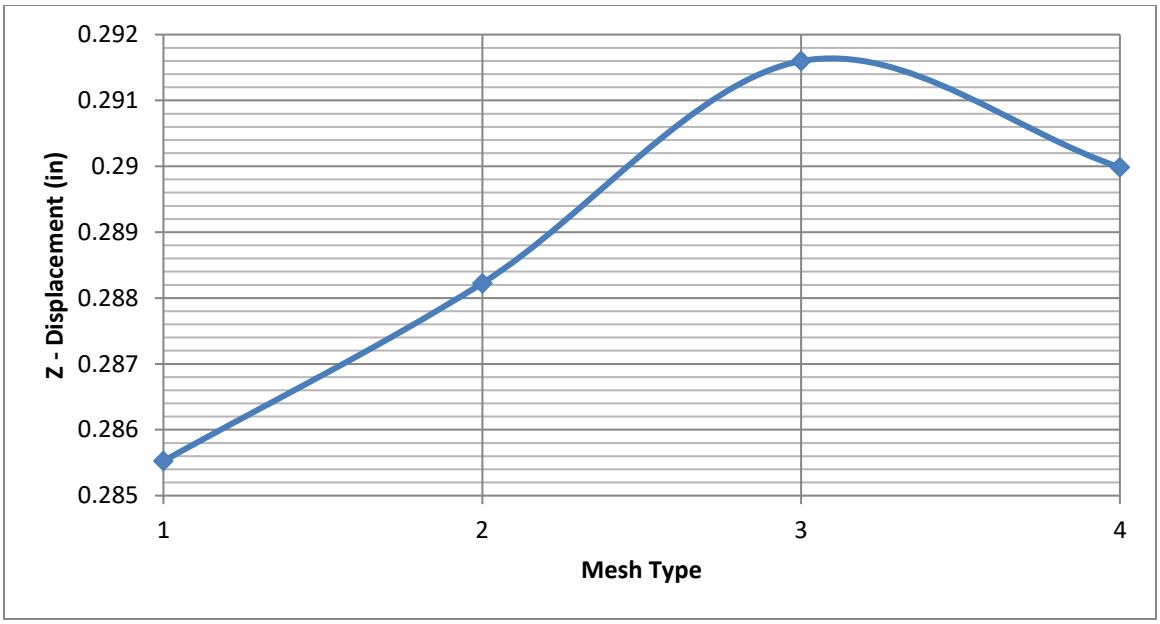

Figure 32. Convergence Study for Downward Z-displacement

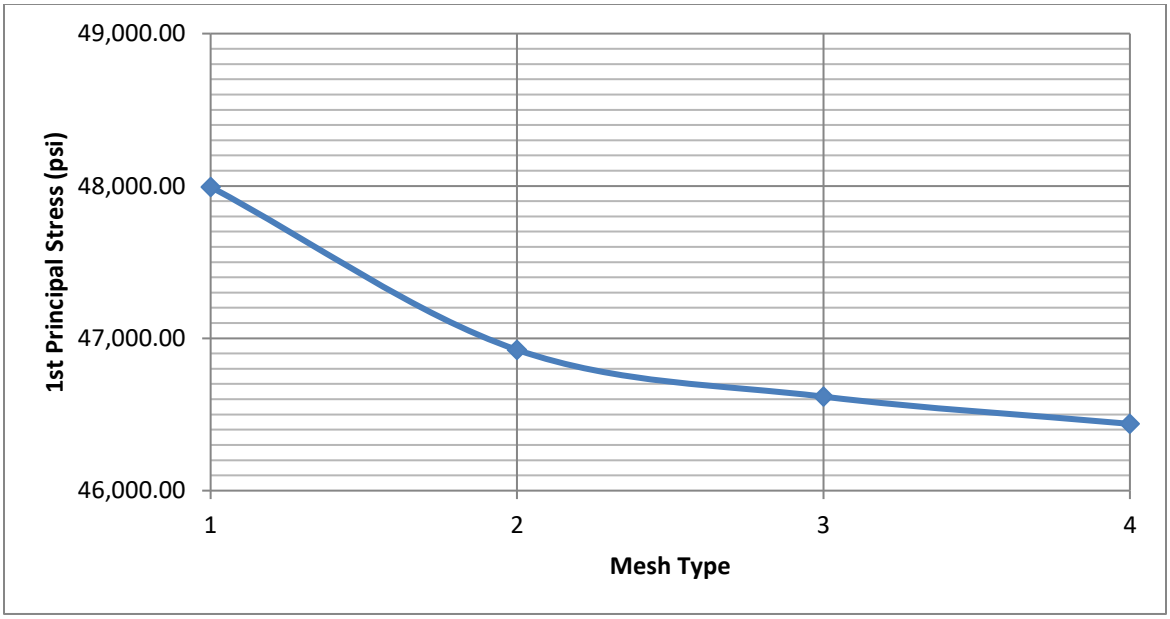

Figure 33. Convergence Study for 1st Principal Stress

The convergence study showed that mesh type 3, with three elements along the glass thickness, provided results that were within 1% of the mesh type 4 results, while having less than half the number of elements of mesh type 4. Therefore, a model with three elements through the glass specimen thickness was used for all remaining computations.

5.1.8. Finite Element Analysis Ultimate Stress & Deflection Results

FEA models for the annealed, heat-strengthened, and fully tempered glass specimens were created. The purpose of the FEA was to generate equations that related experimental loads with specimen maximum deflection and ultimate stress values. The FEA models had identical loading, and support conditions, but varying glass thicknesses. The thicknesses of the glass specimen models matched the average thickness recorded for the annealed, heat-strengthened, and fully tempered specimens, respectively. Measurements of glass specimen thicknesses are shown in Appendix D. Table 11 provides a summary of the FEA simulations for maximum Z-deflection and 1st principal stress. The maximum deflection and stress values were estimated for total loads ranging from 0 to 2000 lb, with 100 lb increments. Graphical representation of load vs deflection, and load vs 1st principal stress results for the annealed, heat-strengthened, and fully tempered glass specimens are shown in Figure 34 - Figure 39.

Table 11. Finite Element Analysis Maximum Z-Deflection and 1st Principal Stress Simulations

	Annealed		Heat-Strengthened		Fully Tempered	
Total Load Applied (lb)	Deflection (in)	Stress (psi)	Deflection (in)	Stress (psi)	Deflection (in)	Stress (psi)
100	0.043	5308	0.043	5289	0.043	5275
200	0.079	10700	0.079	10662	0.079	10634
300	0.113	16002	0.113	15948	0.113	15949
400	0.145	21104	0.144	21037	0.144	20988
500	0.174	25989	0.173	25913	0.173	25851
600	0.201	30568	0.200	30487	0.200	30429
700	0.226	34925	0.225	34839	0.225	34778
800	0.249	39059	0.249	38969	0.248	38908
900	0.272	43006	0.271	42913	0.270	42842
1000	0.293	46784	0.292	46688	0.292	46617
1100	0.313	50401	0.312	50303	0.312	50228
1200	0.333	53886	0.332	53786	0.331	53711
1300	0.352	57250	0.351	57148	0.350	57076
1400	0.370	60508	0.369	60405	0.368	60325
1500	0.388	63667	0.387	63562	0.386	63490
1600	0.405	66741	0.404	66636	0.403	66555
1700	0.422	69744	0.421	69638	0.420	69556
1800	0.438	72692	0.437	72577	0.436	72498
1900	0.454	75568	0.453	75459	0.453	75375
2000	0.471	78396	0.469	78278	0.469	78196

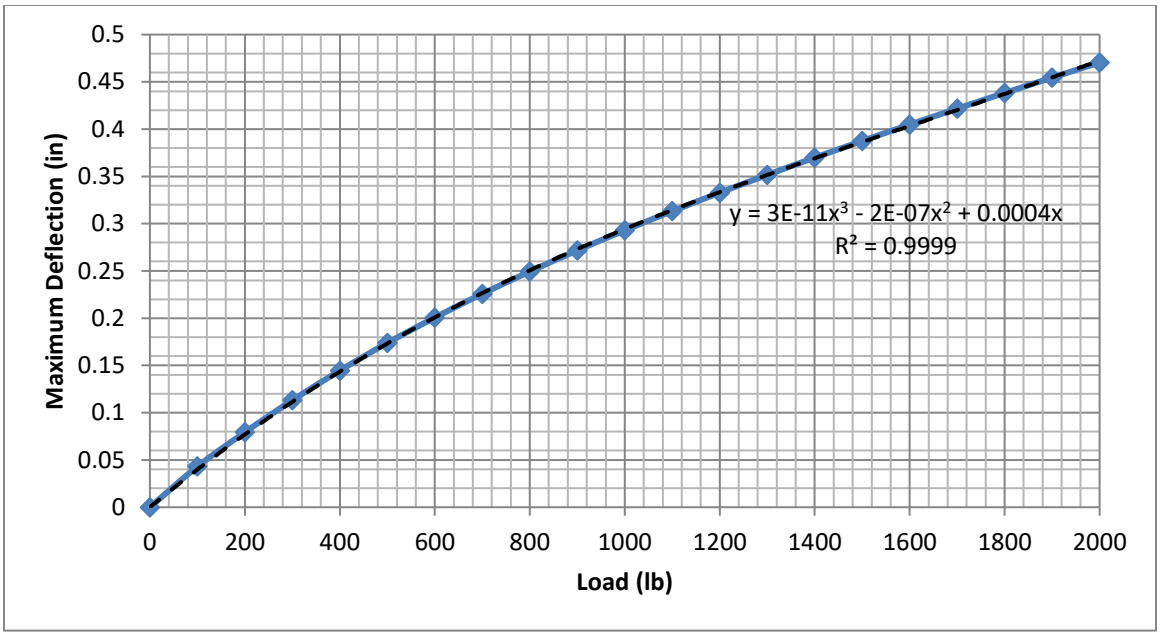

Figure 34. Load vs Deflection Curve for Annealed Specimens

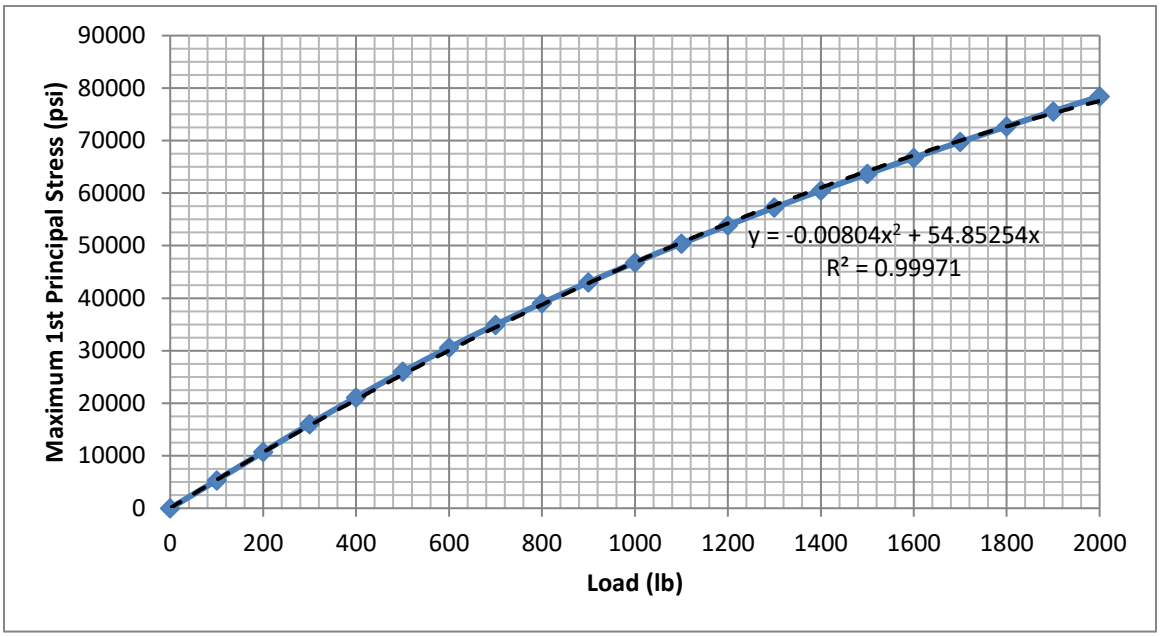

Figure 35. Load vs Stress Curve for Annealed Specimens

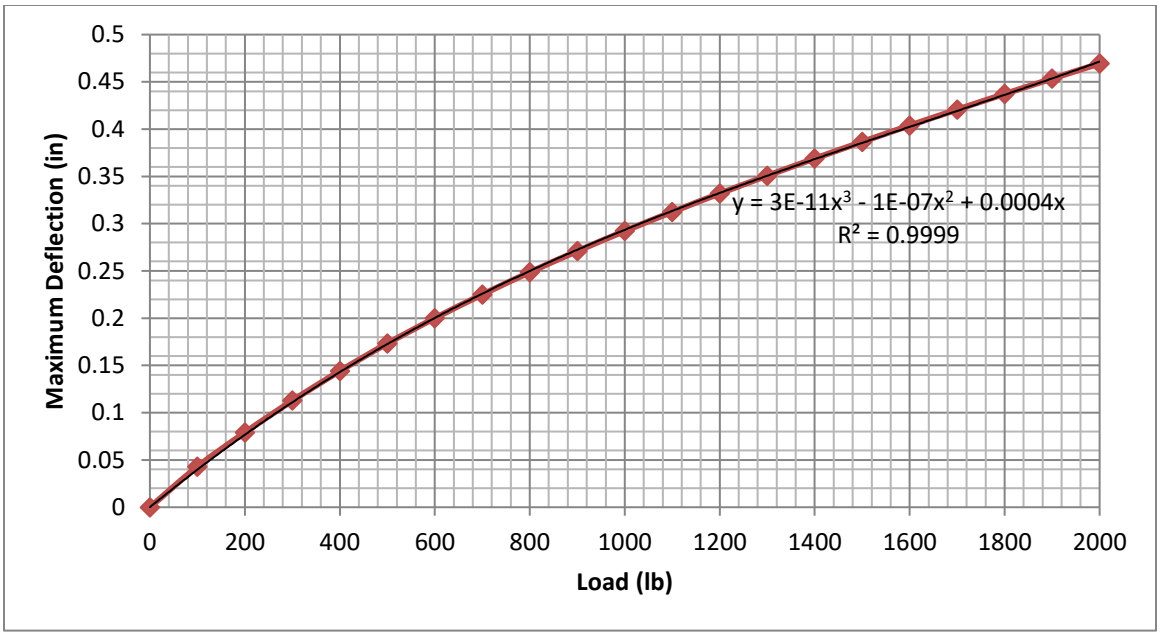

Figure 36. Load vs Deflection Curve for Heat-Strengthened Specimens

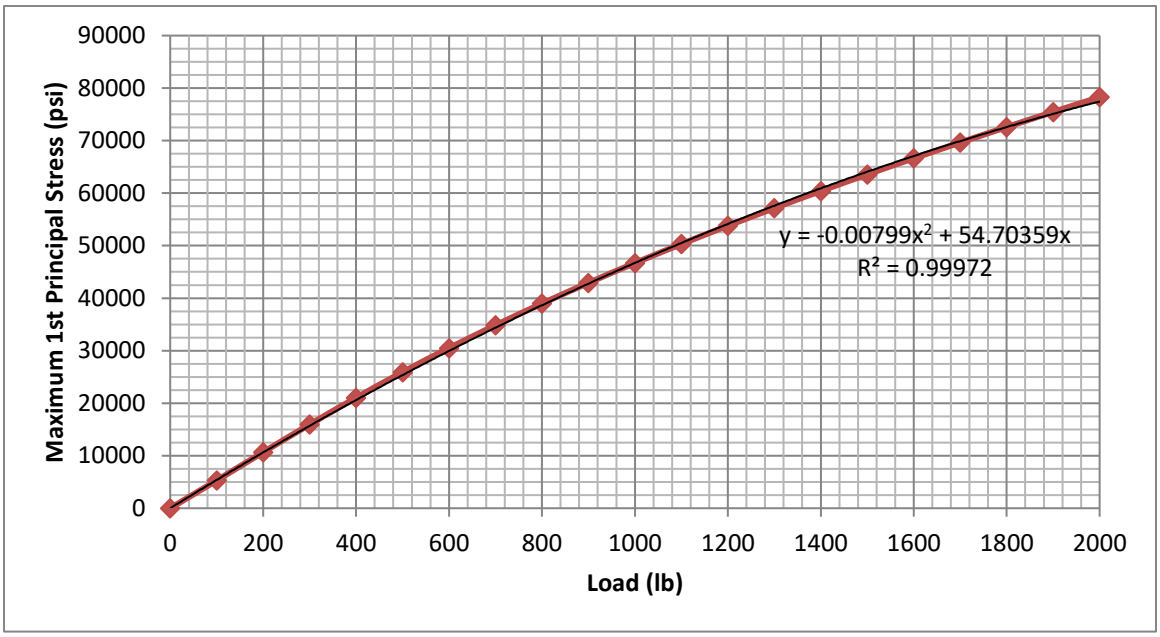

Figure 37. Load vs Stress Curve for Heat-Strengthened Specimens

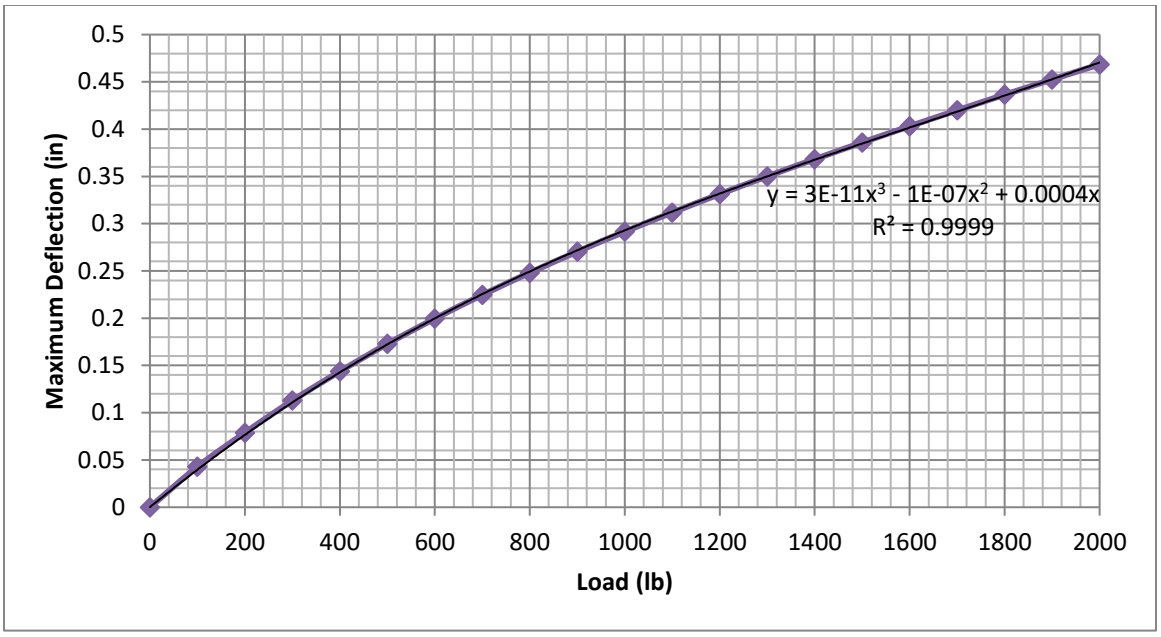

Figure 38. Load vs Deflection Curve for Fully Tempered Specimens

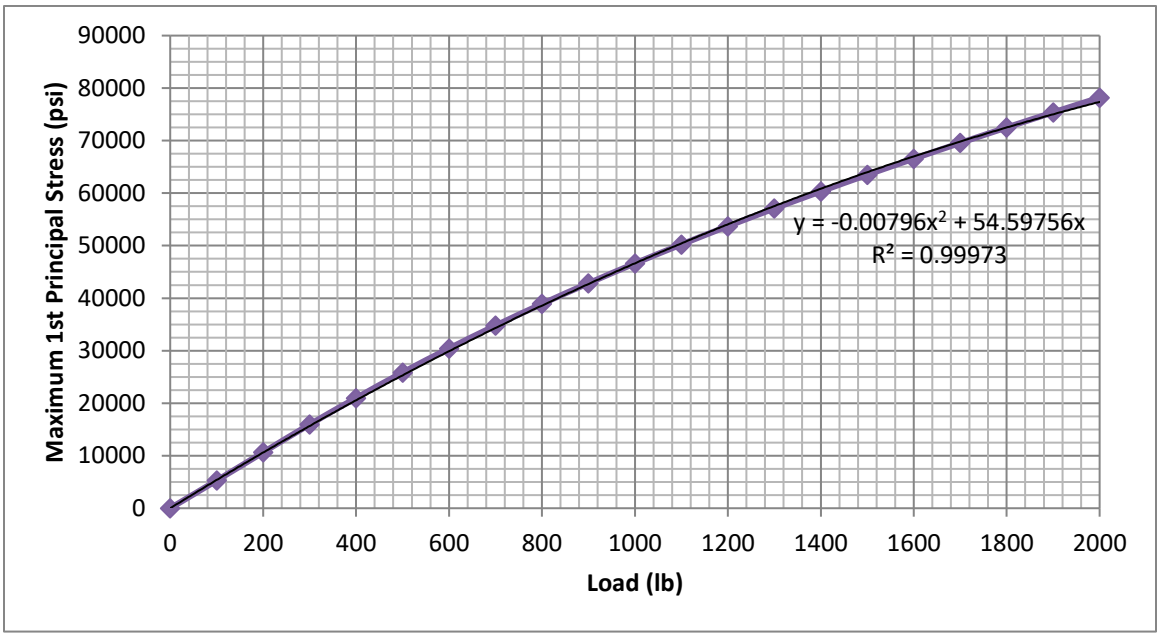

Figure 39. Load vs Stress Curve for Fully Tempered Specimens

The theoretical FEA models developed through ANSYS, indicate that the 1st maximum principal stress in the annealed, heat-strengthened, and fully tempered test specimens can be found through the following equations:

$$\sigma_{ANN-H} = -(8.04 * 10^{-3})P^2 + (54.85)P \quad (5\text{-}6)$$

$$\sigma_{HS-H} = -(7.99 * 10^{-3})P^2 + (54.70)P \quad (5\text{-}7)$$

$$\sigma_{FT-H} = -(7.96 * 10^{-3})P^2 + (54.60)P \quad (5\text{-}8)$$

Where σ_{ANN-H} [psi] is the stress in the annealed glass specimens, σ_{HS-H} [psi] is the stress in the heat-strengthened glass specimens, σ_{FT-H} [psi] is the stress in the fully tempered glass specimens, and P [lb] is the applied load. Values of glass specimen ultimate stresses, which were calculated by entering the experimentally recorded ultimate loads to the above equations, are shown in Table 12.

Table 12. Specimen Ultimate Load and Stress

	Annealed		Heat Strengthened		Fully Tempered	
Specimen Count	Experimental Ultimate Load (lb)	ANSYS Ultimate Stress (psi)	Experimental Ultimate Load (lb)	ANSYS Ultimate Stress (psi)	Experimental Ultimate Load (lb)	ANSYS Ultimate Stress (psi)
1	155	8112	480	23973	521	25846
2	155	8112	521	25898	562	27701
3	155	8112	480	23973	562	27701
4	114	5997	521	25898	521	25846
5	155	8112	521	25898	562	27701
6	155	8112	480	23973	521	25846
7	155	8112	562	27757	521	25846
8	114	5997	439	22051	521	25846
9	155	8112	439	22051	562	27701
10	155	8112	521	25898	562	27701
11	155	8112	480	23973	521	25846
12	155	8112	439	22051	521	25846
13	155	8112	439	22051	562	27701
14	155	8112	439	22051	521	25846
15	155	8112	480	23973	562	27701
16	155	8112	521	25898	562	27701
17	155	8112	439	22051	521	25846
18	155	8112	439	22051	562	27701
19	114	5997	439	22051	562	27701
20	-	-	521	25898	521	25846
21	-	-	480	23973	602	29515

The following section describes the standardized procedures, as presented by Beason and Morgan, which were used to convert the ultimate stress data from Table 12 into ultimate strength data, which are shown as equivalent 3-second load duration failure stresses.

5.2. Equivalent 3-Second Load Duration Failure Stresses

The strength of glass is highly dependent on the duration of loading. ASTM E1300 – *Standard Practice for Determining Load Resistance of Glass in Buildings* defines the strength of glass as the 3-second load duration mean failure stress (ASTM, 2016). A standardized procedure, presented by Beason and Morgan, was used to evaluate equivalent 3-second load duration failure stresses for the glass specimens (Beason and Morgan, 1984). Equation 5-9 expresses the glass resistance to failure, *Kf*, for a specified loading failure as a function of the nominal tensile stress, $\sigma(t)$, load duration, t_f, and a constant, *n = 16*.

$$K_f = \int_0^{tf} [\sigma(t)]^n dt \tag{5-9}$$

Once the magnitude of K_f has been established for a specific loading, Equation 5-9 can be manipulated to solve for the equivalent loading corresponding to any other particular duration as shown in Equation 5-10 below.

$$\tilde{\sigma}_{td} = \left[\frac{\int_0^{td} [\sigma(t)]^n dt}{t_d}\right]^{1/n} \tag{5-10}$$

By substituting t_d for 3-second duration and adjusting the FEA ultimate stresses for the values of residual surface compression, equivalent 3-second duration failure stresses were

estimated. These values are presented in Table 13. Table 14 shows the results of a simple statistical analysis of the equivalent 3-second duration stress data.

Table 13. 3-Second Load Duration Mean Failure Stress Data

	Annealed		Heat Strengthened		Fully Tempered	
Specimen Count	RSC (psi)	3-second Mean Failure Stress (psi)	RSC (psi)	3-second Mean Failure Stress (psi)	RSC (psi)	3-second Mean Failure Stress (psi)
1	-	8959	11014	25573	13712	27098
2	-	8879	10160	26699	14382	28050
3	-	8542	10160	24381	15904	28796
4	-	8234	10160	25910	15119	25607
5	-	6601	10160	25989	15904	27909
6	-	8311	10160	25244	15119	26706
7	-	8327	10160	28378	15904	26964
8	-	8634	10160	21418	15904	25368
9	-	7488	10160	21814	15119	28598
10	-	6337	10574	26009	15904	28602
11	-	7784	10160	24276	15904	27145
12	-	8595	10160	22817	15119	26139
13	-	7826	10160	22690	15904	28930
14	-	7627	10160	22604	15904	26222
15	-	7905	10160	24252	15904	28896
16	-	7563	10160	26164	15904	28315
17	-	8002	10160	22085	15904	25364
18	-	7971	10160	23450	15904	29198
19	-	8955	10160	23439	15119	27847
20	-	-	10160	26868	15119	27232
21	-	-	10160	25583	15904	30155

Table 14. Statistical Overview of the Test Results

	Annealed		Heat Strengthened		Fully Tempered	
	RSC	3-sec Strength (psi)	RSC (psi)	3-sec Strength (psi)	RSC (psi)	3-sec Strength (psi)
Mean (psi)	-	8028	10220	24554	15503	27578
95% Mean CI Limits (psi)	-	7705; 8352	10134; 10306	23742; 25367	15242; 15764	27000; 28157
St Dev (psi)	-	719	203	1899	610	11353
COV (%)	-	8.95	1.99	7.73	3.93	4.91
St Dev of Mean (psi)	-	165	44	414	133	295

At this point, values of residual surface compression and ultimate strength for the annealed, heat-strengthened, and fully tempered glass specimens have been estimated. A discussion on the adequacy of the concept presented in Equation 3-1, to the design of structural glass bolted connections, follows.

5.3. Discussion of Results

Equation 3-1 states that the strength of heat-treated glass equals the strength of annealed glass combined with the residual surface compression from the heat-treating process. This design concept was applied to estimate the strength of the glass specimens considered in this thesis. Figure 40 provides a side-by-side comparison between average specimen strength values measured in this experiment, and average strength values estimated through Equation 3-1. This comparison indicates that the average strength of heat-treated glass specimens estimated through the design concept of Equation 3-1 is ~27% and ~18% lower than the experimentally measured average strength of heat-strengthened and fully tempered glass specimens, respectively. This means that a glass

designer who uses Equation 3-1 in conjunction with FEA to evaluate ultimate stresses in glass plates with mounting holes, would produce a conservative design.

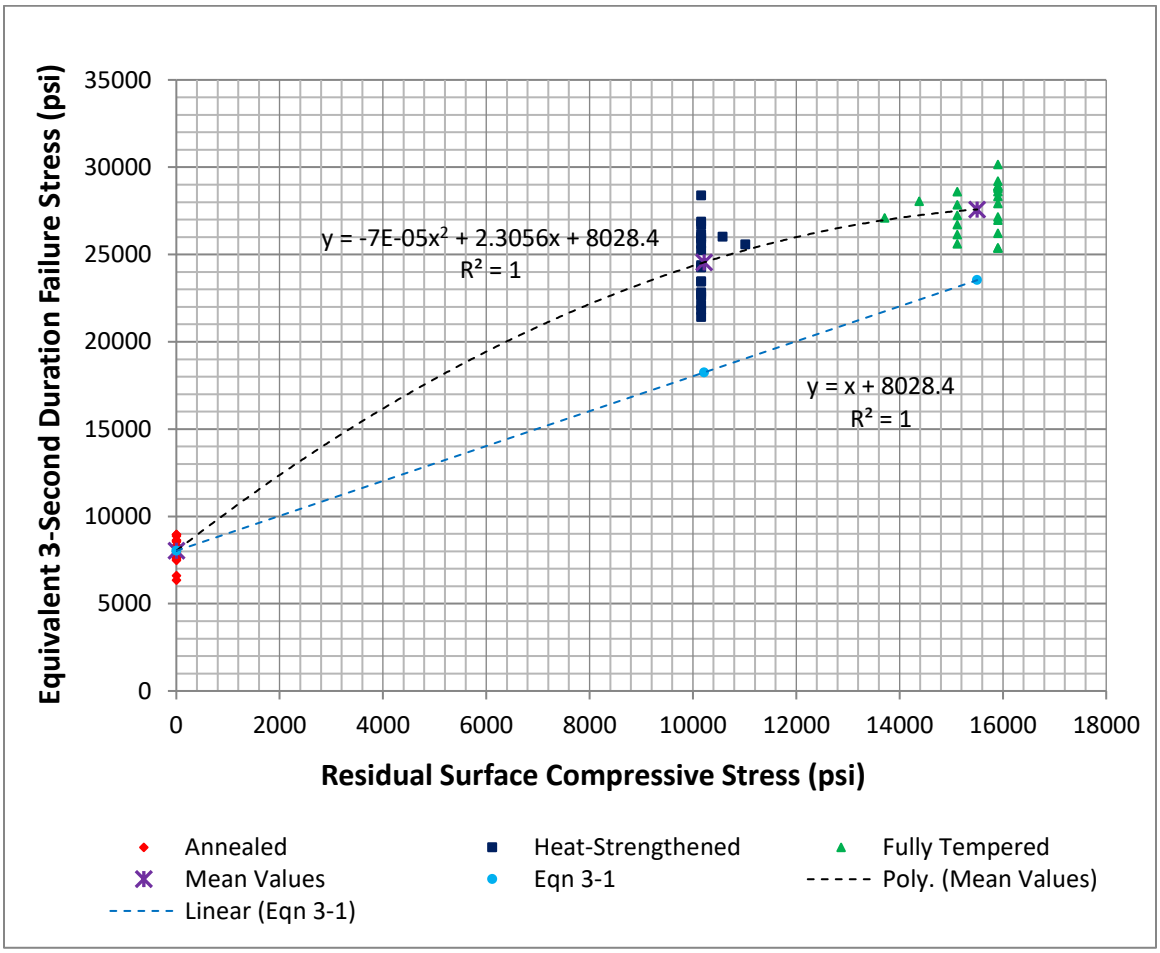

Figure 40. Plot of Residual Surface Compression vs Specimen Ultimate Strength

There are several factors may contribute to the conservatism of Equation 3-1. One factor may be related to the levels of residual surface compression around the mounting hole. In fact, Nielsen, et al. have conducted FEA simulation of residual stresses around glass mounting holes indicate that for thin glass plates, such as the ones considered

herein, levels of residual surface compression in the immediate vicinity of a mounting hole are higher than those away from the mounting hole (Nielsen, et al., 2009).

Another factor that may contribute to the conservatism of Equation 3-1 is the elimination of "weak siblings" during the heat-treatment process. It is believed that any random severe flaws hole-edge flaw in an annealed glass plate would cause the plate to break when subjected to quenching. Therefore, it is likely that the plate specimens that survive the heat-treatment process would have less severe hole-edge flaws.

Lastly, a reason for the conservatism of Equation 3-1 may be related to a possible change of character of hole-edge flaws when subjected to heat-treatment. During the heat-treatment process, the annealed glass plate specimens were heated near their melting point. At that point, it might be reasonable to believe that a portion of the mounting hole-edge flaws may have re-shaped in such a way as to reduce their severity. Thus, the hole-edge flaw characteristics of the final heat-treated plates may have improved during the heat-treatment process.

The following section uses these findings to formulate the conclusions of this research, together with recommendations for future research related to structural glass bolted connections.

6. CONCLUSION & RECOMMENDATIONS

Research discussed in the literature review indicates that the strength of structural glass bolted connections is directly influenced by the residual surface compression in the immediate vicinity of the mounting hole due to the heat-treatment of glass, the localized stress concentration caused by drilling the mounting hole, and the hole-edge condition. Structural glass designers have often estimated the strength of structural glass bolted connections as the summation of the annealed glass strength and the level of residual surface compression induced from the heat-treatment of annealed glass. This design concept is presented in Equation 3-1 of this thesis. The focus of this thesis was to develop an understanding of how the residual surface compression affects the strength of glass around a mounting hole, for a given hole geometry and edge condition. In other words, the focus of this thesis was to understand whether the concept of Equation 3-1 was adequate for the design of structural glass bolted connections.

For that reason, annealed, heat-strengthened, and fully tempered glass plates, with a centered mounting hole, were subjected to destructive testing. Specimen failure loads were recorded and entered into FEA models to estimate specimen ultimate stresses. Specimen ultimate stresses were then adjusted to generate equivalent 3-second duration failure stresses for each type of glass tested. Values of residual surface compression, measured in the heat-strengthened and fully tempered specimens, were paired with the respective specimen's ultimate strength values. This way, a relationship between the measured residual surface compression and the experimental strength of the structural glass bolted connection was established. Lastly, specimen experimental strengths were compared to the theoretical strengths estimated through Equation 3-1.

The following conclusions were drawn from the work presented in this thesis:

1. The use of Equation 3-1 in conjunction with FEA stress results is conservative for the design of structural glass bolted connections.
2. The measured strength of heat-treated glass plates with a centered mounting hole seems to be higher than the strength estimated through Equation 3-1. This change in strength may be a result of a few of phenomena:
    - The higher levels of residual surface compression in the immediate vicinity of the mounting hole than that away from the hole, for the hole geometry considered in this study.
    - The elimination of "weak siblings", which refers to the annealed glass specimens with significant hole-edge flaws that do not survive the heat-treating process.
    - The heat-treatment of annealed glass may affect the character of the flaws in the immediate vicinity of the mounting hole.

Further research, which considers a comprehensive range of glass specimens with various thicknesses and mounting hole characteristics, should be conducted in order to verify the effects of the mounting hole edge conditions to the strength of structural glass bolted connections. If achieved, the quantification of the effects of mounting hole-edge condition to the strength of structural glass bolted connections shall allow for the development of a theoretical model, capable of accurately estimating the strength of structural glass bolted connections.

REFERENCES

ANSYS, Inc. (2013). *ANSYS mechanical APDL element reference*. ANSYS, Canonsburg, PA.

ASM International. (1990). *Metals handbook*. ASM International Handbook Committee, Metals Park, OH.

ASTM International. (2012). *Standard specification for heat-strengthened and fully tempered flat glass*. ASTM Standard C1048-12el, West Conshohocken, PA.

ASTM International. (2016). *Standard practice for determining load resistance of glass in buildings*. ASTM Standard E1300-16, West Conshohocken, PA.

AZOM. (2001). "Properties: Silicone Rubber." *AZoM.com*, <https://www.azom.com/properties.aspx?ArticleID=920>.

Beason, W. L. (1980). "A failure prediction model for window glass." Dissertation, Texas Tech University, Lubbock, TX.

Beason, W. L., and Morgan, J. R. (1984). "Glass failure prediction model." *Journal of Structural Engineering*, 110(2), 197–212.

Beason, W. L., Kohutek, T. L., and Bracci, J. M. (1998). "Basis for ASTM E 1300 annealed glass thickness selection charts." *Journal of Structural Engineering*, 124(2), 215–221.

Beason, W.L., and Lingnell, A.W. (2000). "Emerging uses for window glass." *Emerging Materials for Civil Infrastructure: State of the Art*, R. A. Lopez-Anido and T. R. Naik, eds., ASCE, 190-216.

C. R. Laurence Co., Inc. (2010). "HSFEX14BS - CRL Brushed Stainless Heavy-Duty Exterior Swivel Fastener." *CRL Swivel Fastener-Heavy Duty Fastener*, <http://www.crlaurence.com/crlapps/showline/offerpage.aspx?Productid=88029&GroupID=46002&History=39327:9307:13453:14016&ModelID=46002>.

Davidson, A. (2000). "Glass Ceiling", *Metropolis Magazine*. <http://www.metropolismag.com/html/content_0200/gla.htm>.

Johnson, J., and Holloway, D. (1966). "On the shape and size of the fracture zones on glass fracture surfaces." *Philosophical Magazine*, (14), 731–743.

Khoraskani, R. A. (2015). *Advanced connection systems for architectural glazing*. Springer, New York, NY.

Lindqvist, M. (2013). “Structural glass strength prediction based on edge flaw characterization.” Dissertation, Swiss Federal Institute of Technology, Lausanne, Switzerland.

McLellan, G., and Shand, E. (1984). *Glass engineering handbook*. McGraw-Hill Book Company, New York, NY.

Mitutoyo America Corporation. (2008). *Coolant proof micrometer QuantuMike*, Mitutoyo, Aurora, IL.

Narayanaswamy, O. S. (1971). “A model of structural relaxation in glass.” *Journal of American Ceramic Society*, 54, 491-498.

Nielsen, J. H., Olesen, J. F., Poulsen, P. N., and Stang, H. (2009). “Simulation of residual stresses at holes in tempered glass: a parametric study.” *Materials and Structures*, 43(7), 947–961.

Peterson, R. E. (1974). *Stress concentration factors*. John Wiley & Sons, New York, NY.

Reddy, J. N. (2006). *An introduction to the finite element method*. McGraw-Hill, Boston, MA.

Rodichev, Y., Maslov, V., Netychuk, A., Bodunov, V., and Yevplov, Y. (2007). “Bending strength and fracture of glass materials under the different loading conditions.” *In Glass Performance Days*, pages 615–618.

Sedlacek, G., Blank, K., Laufs,W., and G*u*sgen, J. (1999). *Glas im konstruktiven ingenieurbau*. Ernst & Sohn, Berlin. Germany.

Shand, E. (1959). “Breaking stress of glass determined from dimensions of fracture mirrors.” *Journal of The American Ceramic Society*, 42(10):474–477.

Strainoptics. (2017). *GASP Instruments - For measuring surface stress in tempered, heat-strengthened, and annealed glass*, Strainoptics, North Wales, PA.

Syracuse Glass Company. (2017). *ASTM C1048 tempered glass hole and notch guidelines*. Syracuse Glass, Syracuse, NY.

Timoshenko, S., and Woinowsky-Krieger, S. (1959). *Theory of plates and shells. 2.ed*. McGraw-Hill, New York, NY.

Torres, Y., Bermejo, R., Gotor, F., Chicardi, E., and Llanes, L. (2014). “Analysis on the mechanical strength of WC-Co cemented carbides under uniaxial and biaxial bending.” *Materials & Design*, 55, 851–856.

Vallabhan, C. V. G., and Wang, B. Y-T. (1981). “Nonlinear analysis of rectangular glass plates by finite difference method”. Institute for Disaster Research, Texas Tech University, Lubbock, Tx.

Wang, E., Nelson, T., and Rauch, R. (2004). "Back to elements - tetrahedra vs. hexahedra." Proceedings of International ANSYS Conference, Munich, Germany.

APPENDIX A

This appendix shows the calculation of maximum deflection and bending stress of the cantilever beam problem. This is the first of three problems that were used to verify the FEA capabilities to produce accurate results to structural benchmark problems.

A 12x4x1 glass cantilever beam, where *a* = 12-inch, *b* = 4-inch, and *c* = 1-inch, was loaded on the top surface with a uniform area pressure, *w(z)*, of 1 psi. The area moment of inertia of the beam cross-section, *I*, was calculated first:

$$I_x = \frac{b * c^3}{12} = \frac{4\ in * \ (1\ in)^3}{12} = 0.333\ in^4$$

Applying the Euler-Bernoulli beam theory, the maximum expected displacement, δ_{max}, was computed according to the following equation:

$$\delta_{max} = \frac{w * b * a^4}{8 * E * I_x} = \frac{1\ \frac{lb}{in^2} * 4\ in * (12\ in)^4}{8 * 10.4E6\ \frac{lb}{in^2} * \ 0.333\ in^4} = \ 0.002991\ in$$

The maximum bending moment was found using to be:

$$M = \frac{w * b * a^2}{2} = \frac{1\ \frac{lb}{in^2} * 4\ in * (12\ in)^2}{2} = 288\ lb * in$$

And the maximum bending stress, σ_{max}, experienced by the beam was calculated according to the formula:

$$\sigma_{max} = \frac{M * y}{I_x} = \frac{288\ lb * in * \frac{1}{2}\ in}{0.333\ in^4} = 432\ psi$$

This exact problem was solved in ANSYS. There were two solutions generated: a small deflection solution, which implemented the Euler-Bernoulli beam theory; and a large deflection solution, which took into account the geometric nonlinearity of the problem at hand. In both cases, the solution converged with a mesh of 24x8x2 elements. Figure 41 and Figure 42 present the small and large deflection solution, respectively.

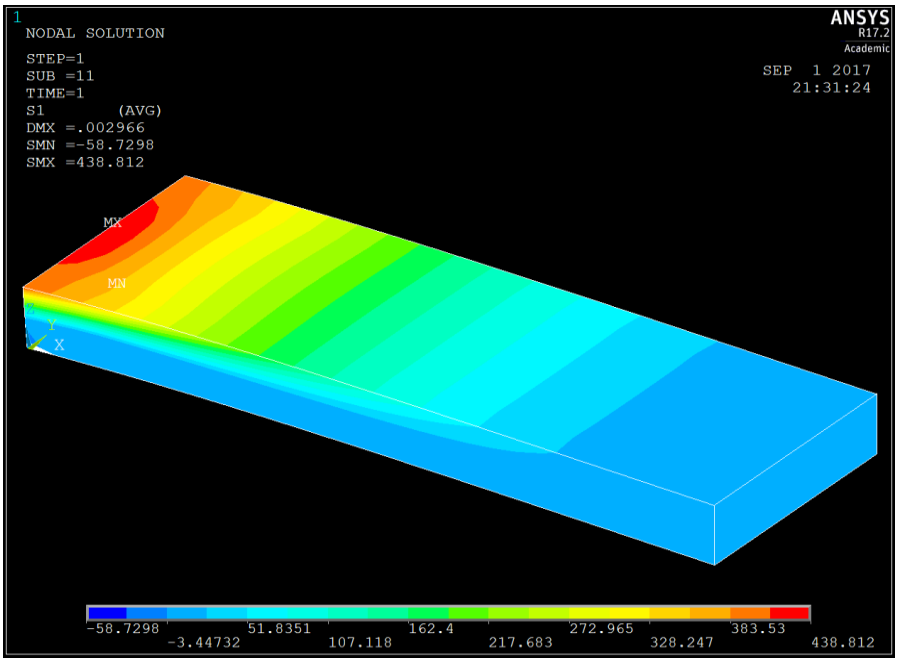

Figure 41. Cantilever Beam 1st Principal Stress - Small Deflection Solution

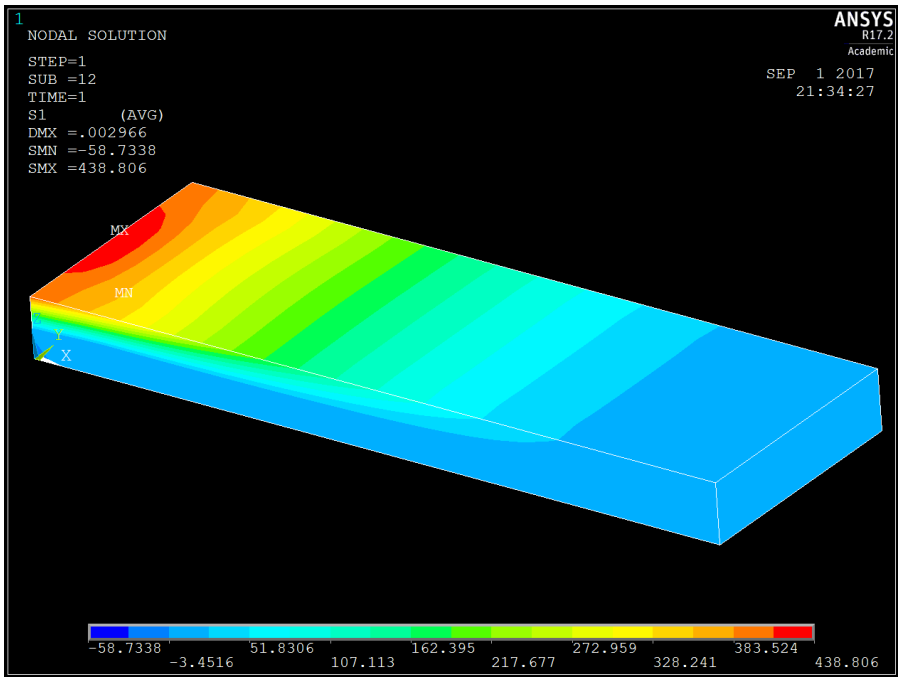

Figure 42. Cantilever Beam 1st Principal Stress - Large Deflection Solution

APPENDIX B

This appendix shows the solution to a simply supported 60x60x1/4-inch glass plate under a lateral uniform area pressure of 0.50 psi. This is the second of three problems that were used to verify the FEA capabilities to produce accurate results to structural benchmark problems.

The ALGOR and ANSYS solutions to the maximum 1st principal stress experienced by the glass plate are presented in Figure 43 - Figure 46.

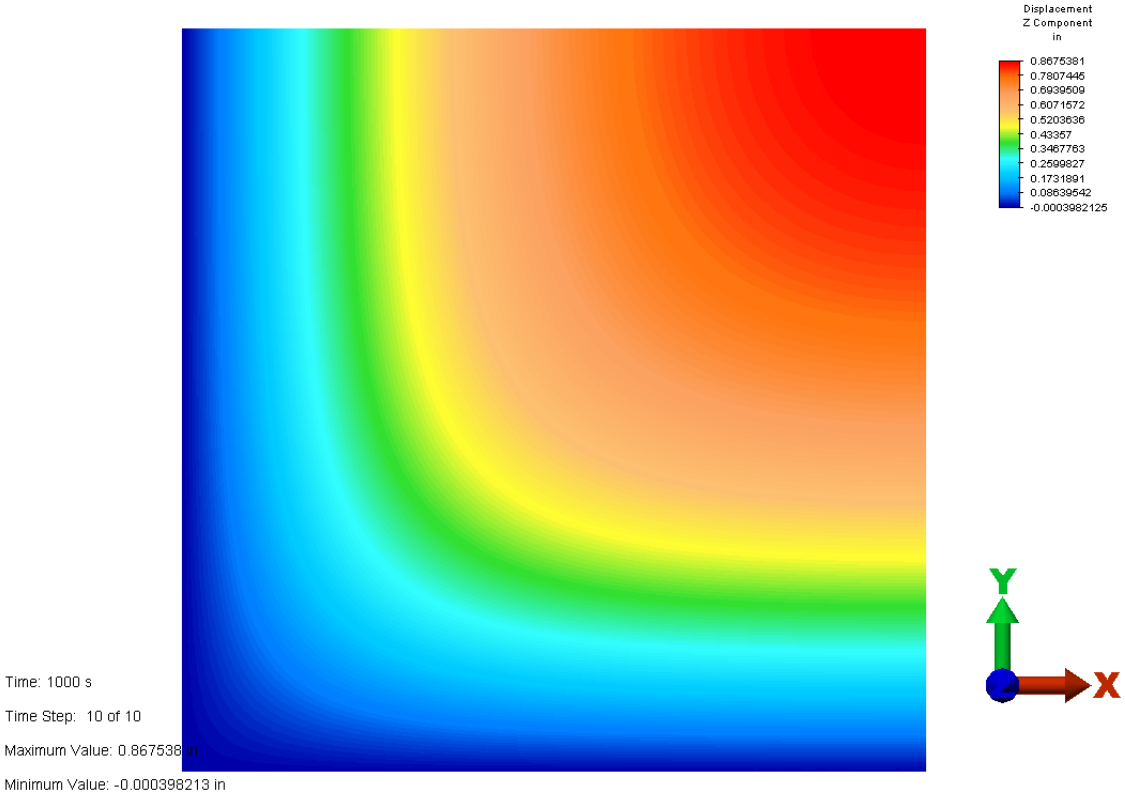

Figure 43. ALGOR Lateral Displacement of the Simply Supported 60x60x1/4" Plate

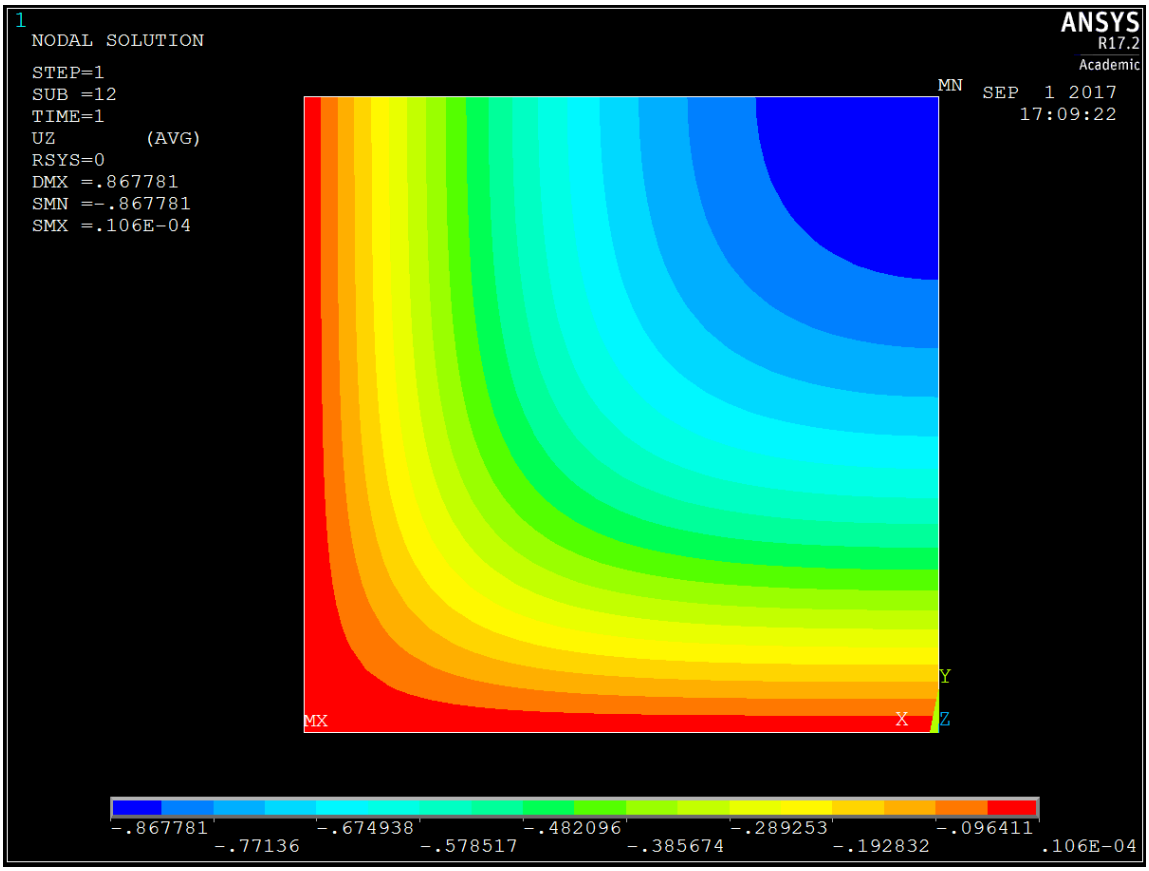

Figure 44. ANSYS Lateral Displacement of the Simply Supported 60x60x1/4" Plate

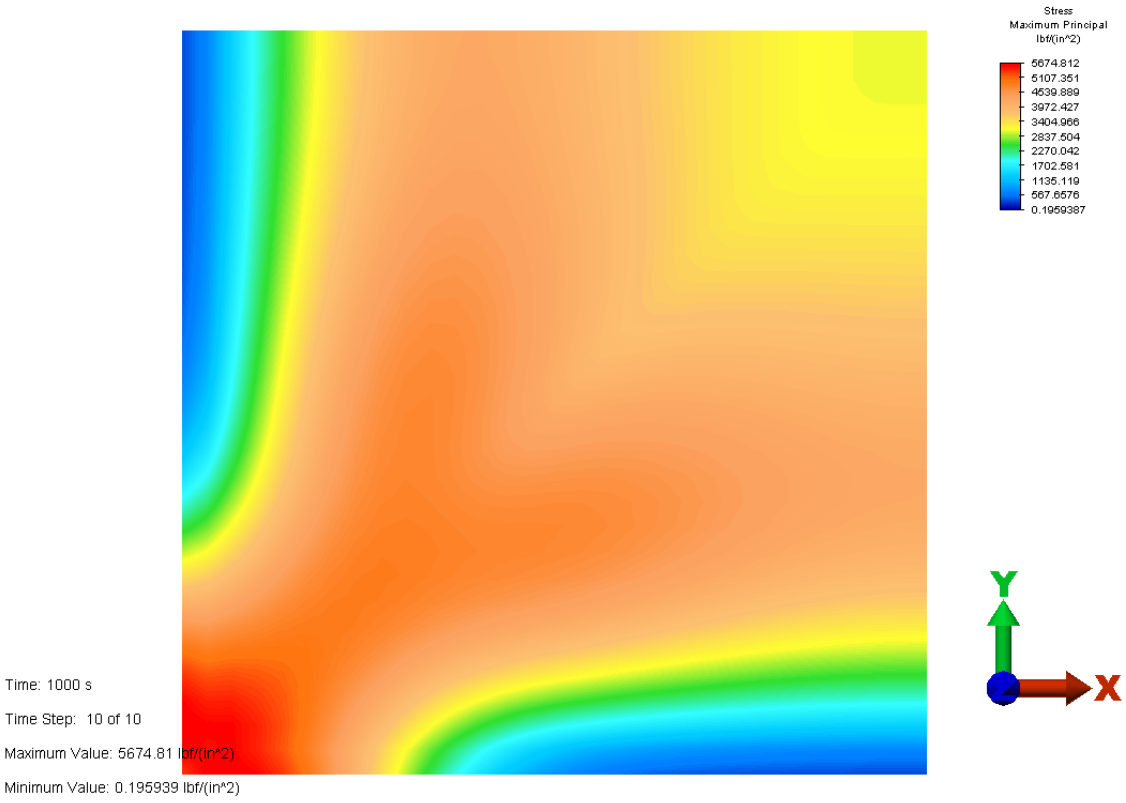

Figure 45. ALGOR 1st Principal Stress of the Simply Supported 60x60x1/4" Plate

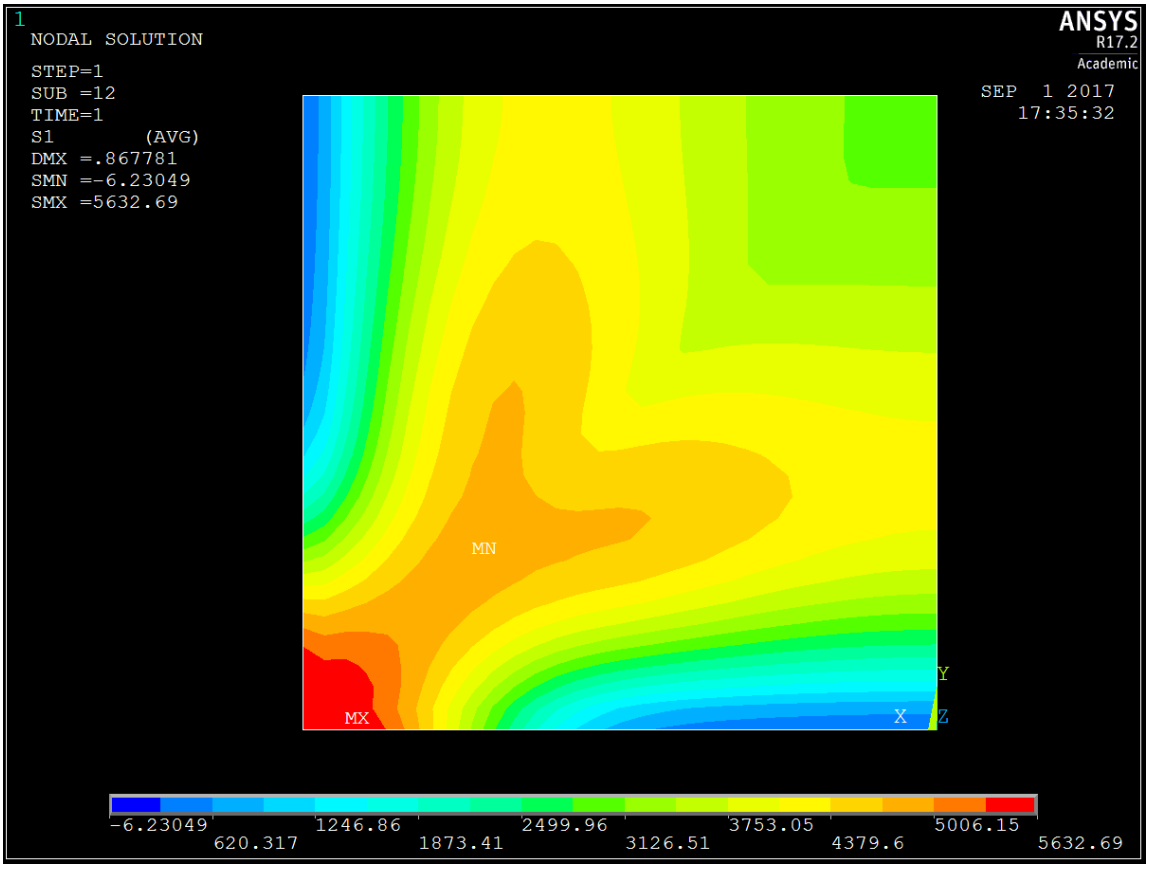

Figure 46. ANSYS 1st Principal Stress of the Simply Supported 60x60x1/4" Plate

APPENDIX C

Appendix C provides the detailed FEA results (Table 15) used to calculate the deflection and stress concentration factors of the FEA model of the glass specimen with a mounting hole. These results were used to verify the FEA capabilities to produce accurate results to structural benchmark problems.

Table 15. Finite Element Model Deflection and Stress Concentration Factors

	Deflection, δ			1st Principal Stress, σ		
Load (lb)	Specimen w/ Hole	Specimen w/out Hole	Deflection Factor, R	Specimen w/ Hole	Specimen w/out Hole	Stress Concentration Factor, Kt
100	0.043 in	0.035 in	1.24	5308 psi	2654 psi	2.00
200	0.079 in	0.068 in	1.17	10700 psi	5304 psi	2.02
300	0.113 in	0.099 in	1.14	16002 psi	7904 psi	2.02
400	0.145 in	0.129 in	1.12	21104 psi	10416 psi	2.03
500	0.174 in	0.156 in	1.11	25989 psi	12815 psi	2.03
600	0.201 in	0.182 in	1.10	30568 psi	15103 psi	2.02
700	0.226 in	0.206 in	1.09	34925 psi	17286 psi	2.02
800	0.249 in	0.229 in	1.09	39059 psi	19371 psi	2.02
900	0.272 in	0.251 in	1.08	43006 psi	21371 psi	2.01
1000	0.293 in	0.271 in	1.08	46784 psi	23286 psi	2.01
1100	0.313 in	0.291 in	1.08	50401 psi	25134 psi	2.01
1200	0.333 in	0.310 in	1.07	53886 psi	26920 psi	2.00
1300	0.352 in	0.329 in	1.07	57250 psi	28651 psi	2.00
1400	0.370 in	0.347 in	1.07	60508 psi	30334 psi	1.99
1500	0.388 in	0.364 in	1.06	63667 psi	31972 psi	1.99
1600	0.405 in	0.381 in	1.06	66741 psi	33569 psi	1.99
1700	0.422 in	0.397 in	1.06	69744 psi	35130 psi	1.99
1800	0.438 in	0.414 in	1.06	72692 psi	36658 psi	1.98
1900	0.454 in	0.430 in	1.06	75568 psi	38220 psi	1.98
2000	0.471 in	0.445 in	1.06	78396 psi	39914 psi	1.96

Similar FEA models were ultimately used to convert experimentally recorded glass specimen failure loads to failure stresses. Thus, it was important to verify that the FEA model incorporated a stress concentration factor that was compatible with Peterson's stress concentration factor. Peterson reports that the stress concentration factor for biaxial bending of an infinite plate with a circular hole is 2 (Peterson, 1974).

Figure 47 and Figure 48 show a graphical representation of the stress and deflection data from Table 15.

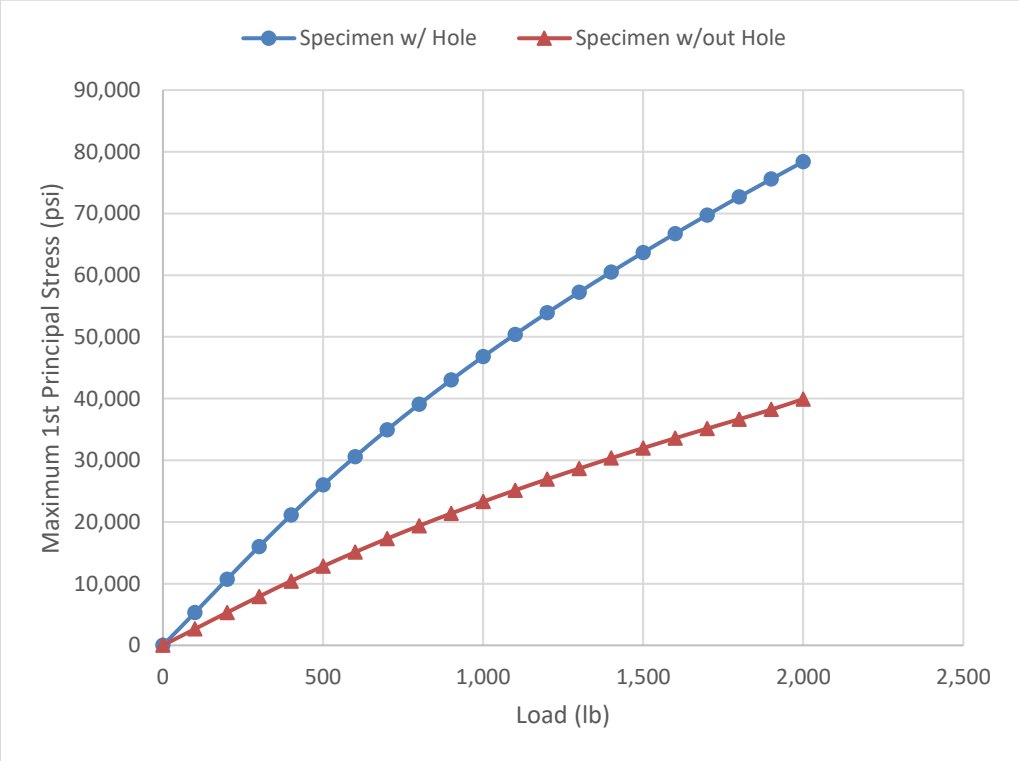

Figure 47. Finite Element Analysis Stress for Model of Glass with and without Mounting Hole

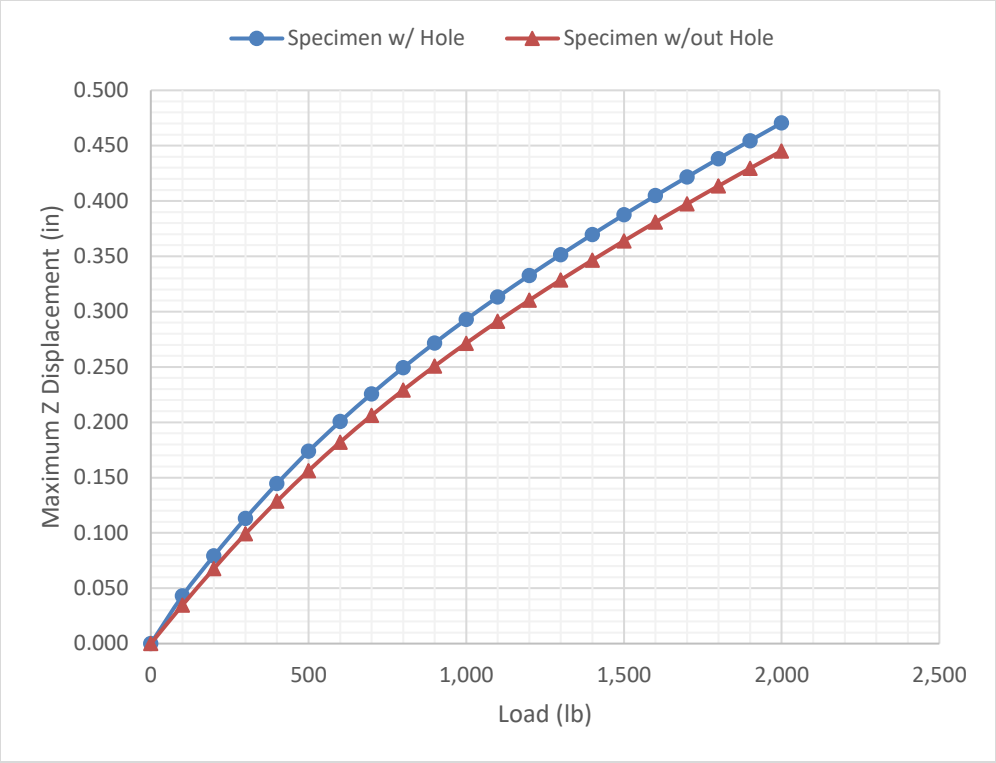

Figure 48. Finite Element Analysis Deflection for Model of Glass with and without Mounting Hole

APPENDIX D

This appendix provides thickness measurements of test specimens. These measurements are reported in Table 16.

Table 16. Measured Thickness of Glass Specimens

Specimen Count	Annealed Glass Thickness (in)	Heat Strengthened Glass Thickness (in)	Fully Tempered Glass Thickness (in)
1	0.22105	0.2215	0.2214
2	0.2224	0.2221	0.2223
3	0.2205	0.2220	0.2222
4	0.2222	0.2218	0.2217
5	0.2211	0.2225	0.2223
6	0.2223	0.2235	0.2257
7	0.22065	0.2235	0.2229
8	0.222	0.2219	0.2251
9	0.2213	0.2233	0.2222
10	0.2221	0.2240	0.2222
11	0.2222	0.2226	0.2223
12	0.2214	0.2216	0.2218
13	0.2218	0.2216	0.2251
14	0.2218	0.2210	0.2222
15	0.2218	0.2249	0.2226
16	0.2217	0.2250	0.2229
17	0.2228	0.2237	0.2229
18	0.2215	0.2214	0.2227
19	0.22305	0.2219	0.2228
20	-	0.2248	0.2222
21	-	0.2225	0.2264